6

Solute Transport

Feike J. Leij
U.S. Salinity Laboratory, USDA-ARS, Riverside, CA

Martinus Th. van Genuchten
U.S. Salinity Laboratory, USDA-ARS, Riverside, CA

6.1 Introduction

Soil scientists and agricultural engineers have traditionally been interested in the behavior and effectiveness of agricultural chemicals (fertilizers, pesticides) applied to soils for enhancing crop growth, as well as in the effect of salts and other dissolved substances in the soil profile on plant growth. More recently, concern for the quality of the vadose zone and possible contamination of groundwater has provided a major impetus for studying solute transport in soils.

The movement and fate of solutes in the subsurface is affected by a large number of physical, chemical and microbiological processes requiring a broad array of mathematical and physical sciences to study and describe solute transport. A range of experimental and mathematical procedures may be employed to quantify transport in soils. Transport of a dissolved substance (solute) depends on the magnitude and direction of the solvent (water) flux; considerable experimental and numerical effort may be needed to determine the transient flow regime in unsaturated soils. Furthermore, the determination of solute concentrations is not always straightforward, particularly if the solute is involved in partitioning between different phases or subject to transformations.

A vast body of work on solute transport can be found in the soil science literature. An equally vast amount of pertinent studies on solute transport in porous media has been published by civil and environmental engineers, geophysicists and geochemists, physical chemists and others. The scope of this chapter permits only an introductory treatment of the subject. First, the standard transport mechanisms pertaining to the fundamental advection-dispersion equation (ADE) will be introduced in Section 6.2. This equation, also known as the convection-dispersion equation, is most often used to model solute transport in porous media. The movement of a solute that undergoes adsorption by the soil requires modifications of the ADE, particularly if several solute species are present that may participate in a number of different reactions. Section 6.3 is devoted to analytical and numerical methods for quantifying solute concentrations as a function of time and space. The traditional advection-dispersion concept is not always adequate to describe solute transport in field soils. Section 6.4 describes the stream tube model as an example of an alternative transport model that may be better suited to model transport in real world situations.

6.2 The Advection-Dispersion Equation

Consider the transport of a chemical species in a three-phase soil-air-water system, and assume that the chemical species (the solute) is completely miscible with water (the solvent). At the macroscopic level and for one-dimensional flow, the mass balance equation for a solute species subject to arbitrary reactions is given as:

$$\frac{\partial \theta C}{\partial t} = -\frac{\partial J_s}{\partial x} + \theta R_s$$

[6.1]

where θ is the volumetric water content ($L^3 L^{-3}$), C is the solute concentration expressed as solute mass-per-solvent volume ($M L^{-3}$), t is time (T), x is position (L), J_s is the solute flux expressed in solute mass-per-cross-sectional area of soil-per-unit time ($M L^{-2} T^{-1}$), and R_s denotes arbitrary solute sinks (< 0) or sources (> 0) ($M L^{-3} T^{-1}$). Similar equations may be derived for multidimensional flow and transport. The solute flux is usually distinguished in an advective and a dispersive component according to:

$$J_S = J_w C + J_D$$

[6.2]

where J_w is a vector quantifying the water flux (LT^{-1}), namely, the Darcian velocity expressed as volume of water-per-cross-sectional area of soil-per-unit time, and J_D is a solute flux to quantify transport caused by a gradient in the solute concentration ($M L^{-2} T^{-1}$), also per unit area of soil.

6.2.1 Transport Mechanisms

The movement of a solute with flowing water, described by the solute flux ($J_w C$), is referred to as advection or convection. Because dissolved substances move in a passive fashion, advective transport can be readily quantified when the solvent flux (J_w) is known. The water flux is generally a function of time and position. However, for transport in laboratory soil columns, J_w is often constant while for field studies, approximations may sometimes be made to facilitate a simpler steady-state one-dimensional flow description.

Even if the macroscopic water flux is known or can be measured, the velocity at smaller pore scales is not easily determined. Variations in the microscopic velocity will lead to unequal solute movement in the direction of flow. This movement is quantified by means of the dispersive solute flux. If, during steady water flow, the solute concentration of the solution at the inlet of a water saturated soil column is changed abruptly at time $t = 0$, the observed breakthrough of a solute at the column outlet at times $t > 0$ will not exhibit an equivalent abrupt change (Nielsen and Biggar, 1961). The solute concentration will change more gradually with time as a result of (hydrodynamic) dispersion, which quantifies the effects of both mechanical dispersion and diffusion. Molecular diffusion and mechanical dispersion will be discussed first for free solutions and then for soil solutions.

6.2.1.1 Diffusion

Molecular or ionic diffusion is an important mechanism for solute transport in soils in directions where there is little or no water flow. A net transfer of molecules of a solute species usually occurs from regions with higher to lower concentrations as the result of diffusion as described by Fick's first law. For a free or bulk solution, the one-dimensional mass flux [J_{dif} ($M L^2 T^{-1}$)] due to molecular diffusion is given by:

$$J_{dif} = -D_o \frac{\partial C}{\partial x}$$

[6.3]

where D_o is the coefficient of molecular diffusion for a free or bulk solution $(L^2 T^{-1})$. Many publications exists that provide data on D_o (Kemper, 1986; Lide, 1995).

The experimentally observed proportionality between J_{dif} and the concentration gradient can be described at the molecular or ionic level with a balance of forces. The driving force for particle movement from higher to lower concentrations is the gradient in the chemical potential. For mixtures with ideal behavior, the chemical potential can be expressed in terms of its mole fraction. For solutions with nonideal mixing behavior, the activity coefficient of the solute needs to be determined. Ionic activity coefficients can be estimated with the extended Debye-Hückel equation or the Davies extension for solutions up to 0.5 M (Section B, Chapter 10). Activity coefficients for a greater concentration range up to 16 M can be estimated with the Pitzer virial equations (Pitzer, 1979; Harvie and Weare, 1980). Codiffusion or counterdiffusion occurs in systems with multiple ion species. Diffusion rates for individual species as predicted solely by Fick's model would violate the electroneutrality principle. The ionic diffusion flux consists then of a term for ordinary Fickian diffusion and a term accounting for electric transference of ions. The corresponding diffusion coefficient is related to the ionic mobility using the Nernst-Planck equation (Helfferich, 1962).

To characterize diffusion in soils, the diffusivity in a free solution is typically adjusted with terms accounting for a reduced solution phase (a smaller cross-sectional area available for diffusion), and an increased path length. A general treatment of diffusion in soils can be found in Olsen and Kemper (1968) and Nye (1979). The macroscopic diffusive flux per unit area of soil can be written as:

$$J_{dif} = -\theta D_{dif} \frac{\partial C}{\partial X}$$

[6.4]

where D_{dif} is the coefficient of molecular or ionic diffusion for the liquid phase of the soil. The diffusion coefficients for the soil liquid and a free liquid are related by (Epstein, 1989):

$$D_{dif} = \frac{D_o}{\left(L_{dif}/L\right)^2} \equiv \frac{D_o}{\tau^2} \equiv D_o \tau_o$$

[6.5]

where L_{dif} and L are the actual and the shortest path lengths for diffusion (L), $\tau = L_{dif}/L$ is known as the tortuosity, and τ^2 as the tortuosity factor, while $\tau_a = (L/L_{dif})^2$ is often designated as an apparent tortuosity factor. The tortuosity L_{dif}/L appears twice in Equation [6.5] to account for changes in the concentration gradient along the streamline and the travel distance as compared to a higher concentration difference and a shorter travel distance along a straight path with length L in a free solution (Olsen and Kemper, 1968). It should be noted that the terms tortuosity and tortuosity factor have not been used consistently in the literature. Furthermore, some authors include the water content in their definition of tortuosity (Dykhuizen and Casey, 1989) or solute adsorption (retardation) in the expression for either τ or D_{dif} (Nye, 1979; Robin et al., 1987).

For unsaturated conditions, it is convenient to quantify the dependency of the diffusion coefficient on water content. Assuming that the tortuosity affects diffusion in the liquid phase in the same way as in the gaseous phase, the tortuosity term previously derived for gaseous diffusion in

soils by Millington (1959) and Millington and Quirk (1961), can be adapted to describe aqueous diffusion in variably saturated soils. The following expressions then result:

$$D_{dif} = \frac{\theta^{10/3}}{\varepsilon^2} D_o \quad , \quad D_{dif} = \frac{\theta^2}{\varepsilon^{2/3}} D_o \qquad [6.6]$$

where ε is the soil porosity ($L^3 L^{-3}$). An equivalent of the first expression, using a volumetric air content instead of θ, has been used frequently to describe gaseous diffusion in soils although Jin and Jury (1996) reported that the lesser known second version provided a better description.

Diffusion coefficients in soil systems are usually determined by mathematically analyzing solute concentration profiles in the soil as a function of time or position. Van Rees et al. (1991) measured diffusivities by allowing diffusion from (1) a spiked solution into a soil having a zero or low initial concentration, (2) a spiked soil into a solution, and (3) a spiked soil into the soil. In the first two procedures, the concentration of the solution is observed as a function of time. A mathematical solution is then fitted to the observation to determine the diffusion coefficient.

The third procedure of diffusion from a soil with a higher to a lower concentration has been widely applied (Kemper, 1986; Oscarson et al., 1992). Two blocks of soil with different concentrations are brought together at time $t = 0$. After sufficient time has elapsed for solute diffusion to occur from the block with the higher to the lower concentration, the joined soil blocks are sectioned. The solute concentration of each section is determined, for example, by using extraction, centrifugation, and chemical analysis of the supernatant liquid. This approach yields a concentration profile versus distance from which the diffusion coefficient may be estimated using an appropriate analytical solution of the governing solute diffusion equation. Consider the diffusion equation,

$$\frac{\partial C}{\partial t} = D_{dif} \frac{\partial^2 C}{\partial x^2} \qquad [6.7]$$

subject to the initial condition,

$$C(x,0) = \begin{cases} C_o & -\infty < x < 0 \\ C_i & 0 < x < \infty \end{cases} \qquad [6.8]$$

and the approximate boundary conditions,

$$C(-\infty, t) = C_o \quad , \quad C(\infty, t) = C_i \qquad [6.9]$$

The solution for this problem is given by (Crank, 1975):

$$C(x, t) = C_i + 0.5(C_o - C_i)\text{erfc}\left(x / \sqrt{4D_{dif}t}\right) \qquad [6.10]$$

where erfc is the complementary error function (Gautschi, 1964). The distributions of the solute concentration as a function of distance for different times after joining two soil blocks with concentrations $C_i = 0$ and C_o, and assuming $D_{dif} = 1 \text{ cm}^2 \text{ d}^{-1}$, are presented in Fig. 6.1.
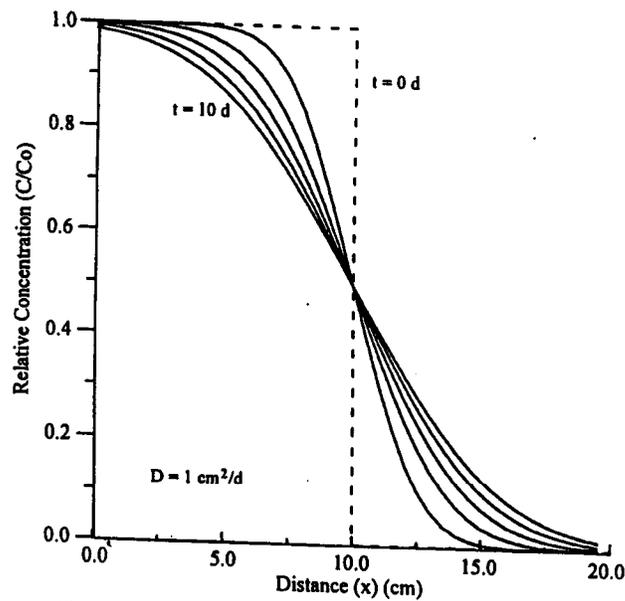
Fig. 6.1 Concentration profiles resulting from diffusion (D_{dif} = 1 d⁻¹) at different times after two soil columns with $C = 0$ and $C = C_o$ were joined at $t = 0$

Typical values for diffusion coefficients in clays and soils with accompanying τ_a are provided in Table 6.1. Additional soil diffusivity data are given by, among others, Hamaker (1972) and Nye (1979).

6.2.1.2 Dispersion

Local variations in water flow in a porous medium will lead to mechanical dispersion. Several mechanisms that are commonly used to contribute to mechanical dispersion are illustrated with hypothetical tracer particles in Fig. 6.2. Dispersion may occur because of (1) the development of a velocity profile within an individual pore such that the highest velocity occurs in the center of the pore, and presumably little or no flow at the pore walls; (2) different mean flow velocities in pores of different sizes; (3) the mean water flow direction in the porous medium being different from the actual streamlines within individual pores, which differ in shape, size, and orientation; and (4) solute particles converging to or diverging from the same pore. All of these processes contribute to increased spreading, in which initially steep concentration fronts become smoother during movement along the main flow direction.

The effects of dispersion can be illustrated with a hypothetical laboratory experiment in which water and a dissolved tracer are applied to an initially tracer-free, uniformly packed soil column of length L (Fig. 6.3). The column is subjected to steady-state water flow with a uniform water content. As more of the tracer is added, the initially very sharp concentration front near the soil surface becomes spread out because of dispersion. Eventually, a smooth and sigmoidally shaped effluent curve can be monitored at the column exit as shown in Fig. 6.3d. In the absence of dispersion, the front of a perfectly inert tracer will travel as a square wave through the column (a process often called piston flow) to reach the bottom of the column at time $t = L/v$, where v is the average pore water or interstitial velocity. This velocity is the ratio of the Darcian water flux density (J_w), and the volumetric water content (θ). Notice that v is given per unit area of fluid whereas J_w is defined per unit area of (bulk) soil.

Table 6.1 Selected diffusion coefficients for aqueous solutions in clay and soil materials

D_o cm^2 day^{-1}	τ_a -	ρ_b g cm^{-3}	Comments
van Rees et al. (1991)†			
1.46	0.64	1.42	spiked water on top of sediment ($\theta = 0.42$)
1.47	0.70	1.42	spiked water on top of sediment ($\theta = 0.42$)
1.66	0.79	1.35	spiked water on top of sediment ($\theta = 0.45$)
1.46	0.69	1.35	lake water on top of spiked sediment ($\theta = 0.45$)
0.97	0.46	1.42	sediment on top of spiked sediment ($\theta = 0.42$)
Robin et al. (1987)‡			
0.19	0.11	1.63	25 °C
0.20	0.11	1.61	25 °C
0.36	0.11	1.62	60 °C
0.40	0.12	1.61	60 °C
0.54	0.11	1.63	90 °C
0.56	0.11	1.64	90 °C
Oscarson et al. (1992)§			
0.33	0.19	0.90	
0.27	0.15	1.12	
0.17	0.10	1.31	
0.08	0.05	1.50	

† ^3H_2O tracer in litoral sediment

‡ ^{36}Cl tracer in bentonite-sand mixture using a spiked ($C_o \approx 0.27\ M$) and unspiked soil plug for different temperatures

§ ^{125}I tracer in compacted bentonite using spiked and unspiked clay plugs

For piston flow, the tracer reaches the column exit exactly after one pore volume of tracer solution has been injected (or collected at the column exit). Pore volume is defined as the amount of water stored in that column.

The degree of spreading is usually related to the solute travel time, although some constraints do exist on the amount of spreading. Dispersion, as sketched in Fig. 6.2a, is limited because of transverse molecular diffusion which causes solutes to move from the center of a tube to areas near the pore walls, or *vice versa*, in response to local concentration gradients. Such transverse diffusion counteracts spreading caused by variations in the longitudinal flow velocity. Dispersion is also limited since capillaries in a porous medium generally are not independent cylindrical tubes, but branch and join or rejoin each other at distances characteristic of the pore or particle size distribution of the medium. This branching and rejoining promotes lateral mixing of solutes from different pores as sketched in Fig. 6.2d.

The macroscopic solute flux due to mechanical dispersion is often conveniently described by Fick's first law of diffusion, despite the conceptual differences between the diffusion and dispersion mechanisms (Scheidegger, 1974). A mathematical foundation for the Fickian description of mechanical dispersion is provided in a classical paper by Taylor (1953). He considered a circular tube, with tube radius r_o (L), filled with water flowing according to a parabolic velocity profile, with v_o being the maximum velocity at the axis (L T^{-1}) and a mean velocity $<v> = v_o/2$ over a cross-section of the tube. Taylor (1953) obtained the following expression for the coefficient of mechanical dispersion:

(a)

(b)

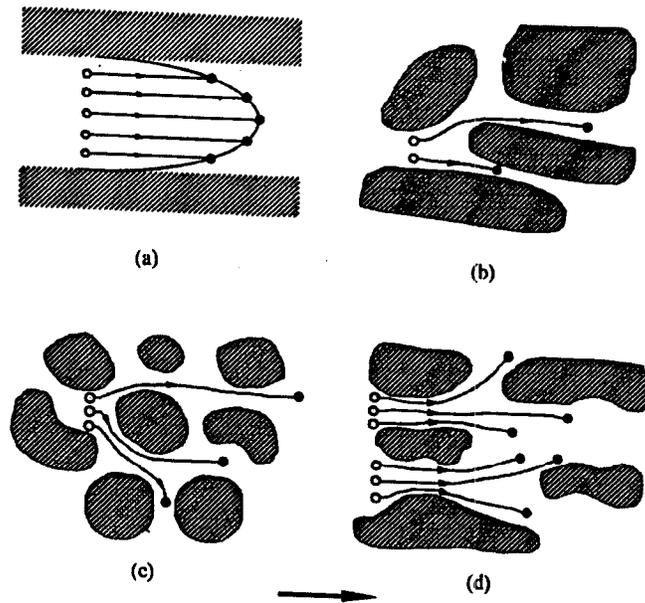(c)

(d)

Direction of average flow

Fig. 6.2 Schematic concepts contributing to mechanical dispersion

1.0

C/C₀ 0.5 (b)

Influent

0

Time (d)

(a)

C/C₀

0.00 0.5

t = 0.2 d

0.25 0.6

0.50 1.0

0.75 1.4

1.00

Depth (m)

(c)

Effluent
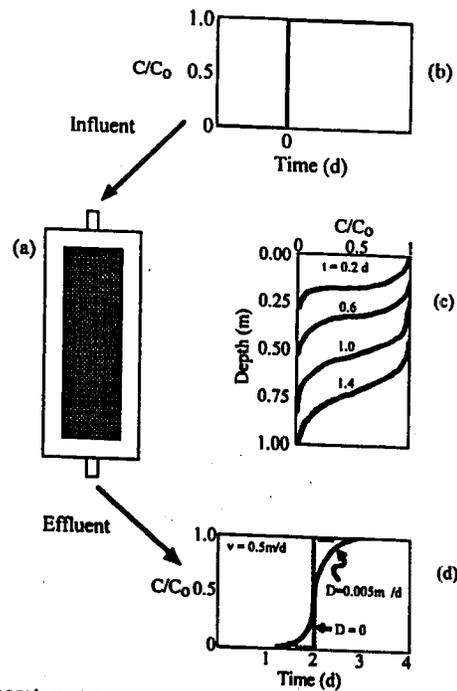
1.0

v = 0.5m/d

C/C₀ 0.5

D=0.005m /d

D = 0

0

1 2 3 4

Time (d)

(d)

Fig. 6.3 Hypothetical laboratory tracer experiment: (a) column of soil, (b) influent curve, (c) concentration distributions inside the column, and (d) breakthrough curves with and without dispersion [Modified after van Genuchten, 1988. p. 360-362. *In* S.P. Parker (ed.) McGraw-Hill Yearbook of Science and Technology, McGraw-Hill, New York]

$$D_{dis} = \frac{r_o^2 v_o^2}{192 D_o} = \frac{r_0^2 <v>^2}{48 D_o}$$

[6.11]

which is valid after sufficient time has elapsed. Note that D_{dis} ($L^2 T^{-1}$) is inversely proportional to the coefficient of molecular diffusion, D_o. The results by Taylor were later derived by Aris (1956) for more general conditions.

Because of the complex geometry of the pore space, microscopic flow and transport processes in soils do not easily lend themselves to a relatively simple analysis as is possible for solute transport in a well-defined, water-filled pore. Dispersion in soils can only be approximately described as a Fickian process, particularly at the early stage of solute displacement in which case other models may need to be employed (Jury and Roth, 1990).

The one-dimensional solute flux due to mechanical dispersion in a uniform isotropic soil may be approximated in a similar way as Fick's law:

$$J_{dis} = -\theta D_{dis} \frac{\partial C}{\partial x}$$

[6.12]

where J_{dis} is the dispersive solute flux (M L^{-2} T^{-1}).

The above one-dimensional geometry may be too simplistic for many transport problems. Three-dimensional dispersion is quantified with a dispersion tensor. The components of the symmetric dispersion tensor for an isotropic soil are given as (Bear and Verruijt, 1987):

$$D_{ij} = \delta_{ij}\alpha_T|\vec{v}| + (\alpha_L + \alpha_T)v_i v_j / |\vec{v}|$$

[6.13]

where $|\vec{v}|$ denotes the magnitude of the pore water velocity with v_i as the ith component (LT^{-1}), δ_{ij} is the Kronecker delta ($\delta_{ij} = 1$, if $i = j$ and $\delta_{ij} = 0$, if $i \neq j$), and α_L and α_T are, respectively, the longitudinal and transverse dispersivity (L). For a one-dimensional system, Equation [6.13] reduces to $D_{dis} = \alpha_L|v|$. Mechanical dispersion, as sketched in an idealized fashion in Fig. 6.2a, can be reversed by changing the flow direction to make a smooth front steep again. In soils, however, dispersion is not reversible since mixing erases antecedent concentration distributions, as illustrated in Fig. 6.2d. Absolute values are, therefore, used for v in Equation [6.13].

In the case of uniform water flow parallel to the x-axis of a Cartesian coordinate system, only the following three main components of Equation [6.13] need to be considered:

$$D_{xx} = \alpha_L v \quad , \quad D_{yy} = \alpha_T v \quad , \quad D_{zz} = \alpha_T v$$

[6.14]

where D_{xx} is the coefficient of longitudinal (mechanical) dispersion, and D_{yy} and D_{zz} are the coefficients of transverse dispersion. This relationship is similar to that derived by Taylor since $<v>$ is inversely proportional to r_o^2 in Equation [6.11].

The macroscopic similarity between diffusion and mechanical dispersion has led to the practice of describing both processes with one coefficient of hydrodynamic dispersion ($D = D_{dis} + D_{dif}$). This practice is consistent with results from laboratory and field experiments which do not permit a distinction between mechanical dispersion and molecular diffusion. The hydrodynamic dispersive flux (J_D) (Equation [6.2]) consists of contributions from molecular diffusion (Equation [6.4]) and mechanical dispersion (Equation [6.12]):

$$J_D = J_{dif} + J_{dis} \tag{6.15}$$

Since diffusion is independent of flow, the contribution of diffusion to hydrodynamic dispersion diminishes if the soil water flow rate increases. Hydrodynamic dispersion is often simply referred to as dispersion, as will be done in the remainder of this chapter.

Dispersion coefficients may be determined by fitting a mathematical solution to observed concentration (Toride et al., 1995). Additional procedures to determine dispersion coefficients are given by Fried and Combarnous (1971) and van Genuchten and Wierenga (1986). Values of the longitudinal dispersivity (α_L) for laboratory experiments typically vary between 0.1 and 10 cm with six to 20 times smaller values for α_T (Klotz et al., 1980). Dispersivities for field soils are generally much higher. Gelhar et al. (1992) reviewed published field-scale dispersivities determined in aquifer materials that are typically one or two orders of magnitudes larger, even more so for relatively large experimental scales.

6.2.2 Advection-Dispersion Equation

The expressions for the advective and dispersive solute fluxes can be substituted in mass balance Equation [6.1]. The one-dimensional advection-dispersion equation for solute transport in a homogeneous soil becomes:

$$\frac{\partial \theta C}{\partial t} = -\frac{\partial}{\partial x}\left(J_w C - \theta D \frac{\partial C}{\partial x}\right) + \theta R_s \tag{6.16}$$

In the case where the water content is invariant with time and space, the ADE may be simplified to ($v = J_w/\theta$):

$$\frac{\partial C}{\partial t} = D \frac{\partial^2 C}{\partial x^2} - v \frac{\partial C}{\partial x} + R_s \tag{6.17}$$

This is a second order linear partial differential equation. Similar to the diffusion equation, the ADE is classified as a parabolic differential equation. To complete the mathematical formulation of the transport, several concentration types and mathematical conditions will be reviewed in Section 6.3.1.

A variety of solute source or sink terms may be substituted for R_s. The most common source/sink term is due to adsorption/desorption and ion exchange stemming from chemical and physical interactions between the solute and the soil solid phase. Many other processes such as radioactive decay, aerobic and anaerobic transformations, volatilization, photolysis, precipitation/dissolution, reduction/oxidation, and complexation may also affect the solute concentration. A further refinement of the transport model is necessary in the case of nonuniform interactions between the solute and the soil, or if there is adsorption on moving particles and colloids. In the following, only interactions at the solid-liquid interface will be considered.

6.2.3 Adsorption

Dissolved substances in the liquid phase can interact with several soil constituents such as primary minerals, oxides, and inorganic or organic colloids. Dissolved ions in the soil solution counterbalance the surface charge of soil particles caused by isomorphous substitution of one element for another in

the crystal lattice of clay minerals, by the presence of hydronium or hydroxyl ions at the solid surface, or other mechanisms. The net surface charge of an assemblage of soil particles produces an electric field that affects the distribution of cations and anions within water films surrounding the soil particles. The mechanisms and characteristics of reactions in solid-solution-solute systems are further discussed in Section B, Chapter 3.

Adsorption of solute (adsorbate) by the soil (adsorbent) is an important phenomenon affecting the fate and movement of solutes. The ADE for one dimensional transport of an adsorbed solute may be written as:

$$\frac{\partial C}{\partial t} + \frac{\rho_b}{\theta}\frac{\partial S}{\partial t} = D\frac{\partial^2 C}{\partial x^2} - v\frac{\partial C}{\partial x}$$

[6.18]

where S is the adsorbed concentration, defined as mass of solute per mass of dry soil (M M^{-1}). The above equation can be expressed in terms of one dependent variable by assuming a suitable relationship between the adsorbed and liquid concentrations. This is typically done with a simple adsorption isotherm to quantify the adsorbed concentration as a function of the liquid concentration at a constant temperature. In addition to temperature, the adsorption isotherm is generally also affected by the solution composition, total concentration, the pH of the bulk solution, and sometimes the method used for measuring the isotherm. A mathematically pertinent distinction is often made between linear and nonlinear adsorption. Although most adsorption isotherms are nonlinear, the adsorption process may often be assumed linear for low solute concentrations or narrow concentration ranges.

6.2.3.1 Linear Adsorption

Consider the general case of nonequilibrium adsorption, where a change in C is accompanied by a delayed change in S. The adsorption rate can be described assuming first order kinetics:

$$\frac{\partial S}{\partial t} = kh(C, S)$$

[6.19]

where k is a rate parameter (T^{-1}) and h is a function to quantify how far the adsorption or desorption process is removed from equilibrium. A single-valued isotherm for equilibrium adsorption $\Gamma(C)$ as in Equation [6.24], is used to define $h(C,S)$ according to:

$$h(C, S) = \Gamma(C) - S$$

[6.20]

For equilibrium adsorption $k \to \infty$, and hence $h(C,S) \to 0$, which implies that $S = \Gamma(C)$. For a linear adsorption isotherm, the relation between Γ and C can simply be given as:

$$\Gamma = K_d C$$

[6.21]

where K_d is a partition coefficient, often referred to as the distribution coefficient, expressed in volume of solvent per mass of soil (L^3 M^{-1}). For $\Gamma = S$, substitution of Equation [6.21] into Equation [6.18] leads to the following ADE commonly used to describe transport of a solute that undergoes linear equilibrium exchange:

$$R\frac{\partial C}{\partial t} = D\frac{\partial^2 C}{\partial x^2} - v\frac{\partial C}{\partial x}$$

[6.22]

in which the retardation factor R is given by

$$R = 1 + \frac{\rho_b}{\theta}K_d$$

[6.23]

with ρ_b as soil bulk density. The advective and dispersive fluxes are reduced by a factor R as a result of adsorption. The movement of the solute is said to be retarded with respect to the average solvent movement. If there is no interaction between the solute and the soil ($K_d = 0$), the value for R is equal to unity. The value for R can be readily calculated from K_d as obtained from chemical analyses of the solution and adsorbed phases. Alternatively, R can be estimated from solute displacement studies on laboratory soil columns (Fig. 6.3). A mathematical solution may then be used to estimate R from observed concentrations with nonlinear optimization programs. The change in the amount of solute in the soil column should be equal to the net solute flux into the column; the following mass balance can hence be formulated to estimate R:

$$v[g(t) - C_e] = R\int_0^L [C(x,t) - f(x)]dx$$

[6.24]

where C_e is the effluent concentration and $f(x)$ and $g(t)$ are the initial and influent concentrations.

The effects of linear adsorption on solute transport in a homogeneous soil profile are shown in Fig. 6.4. Analytically predicted solution and adsorbed concentrations are plotted four days after the start of a one-day application of influent with a unit solute concentration (units may be selected arbitrarily) to an initially solute-free soil profile subject to steady saturated water flow. Other parameters for this example are $J_w = 10$ cm d^{-1}, $\theta = 0.40$ cm^3 cm^{-3}, and $D = 62.5$ cm^2 d^{-1}. The pore water velocity ($v = J_w/\theta$) is hence 25 cm d^{-1} and $\alpha_L = 2.5$ cm. Solute distributions are plotted (Fig. 6.4) for three values of the retardation factor, R. When R is increased from 1.0 to 2.0, the apparent solute velocity (v/R) is reduced
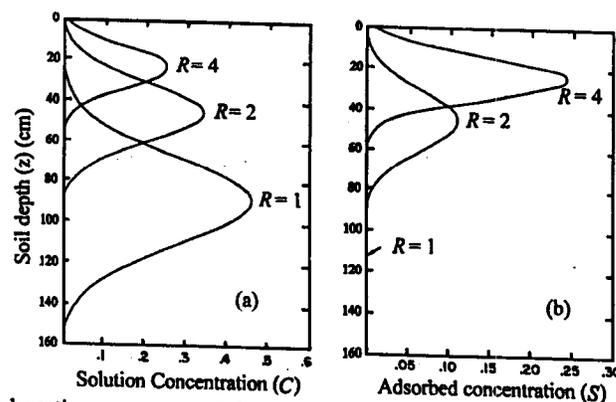

Fig. 6.4 Effect of adsorption, as accounted for by the retardation factor R, on solution (C) and adsorbed (S) concentration distributions in a homogeneous soil profile

by one-half (Fig. 6.4a), causing a shallower penetration of the solute pulse into the profile. At the same time, the area under the curve in Fig. 6.4a is also reduced by one-half. When $R = 4$, the apparent solute velocity and the area under the curve are again reduced by half. Distributions for the adsorbed concentration (S) which increases from zero (no adsorption) when $R = 1$ to a maximum when $R = 4$ are similar (Fig. 6.4b). Assuming a soil bulk density (ρ_b) of 1.25 g cm^{-3} and the same water content as before ($\theta = 0.40$ cm^3 cm^{-3}), one may calculate, using Equation [6.23], that the distribution coefficient K_d = 0, 0.32 and 0.96 cm^3 g^{-1} for $R = 1, 2,$ and 4, respectively.

Anion exclusion occurs when negatively charged surfaces of clays and ionizable organic matter are present; anions are repelled from such surfaces and accumulate in the center of pores. Because water flow velocities are zero at pore walls and maximum in the center of pores (Fig. 6.2a), the average anion movement will be faster than the average water movement. Many displacement experiments also suggest faster anion than water movement simply because the apparent displacement volume is smaller for anions than water. The quantity $(1-R)$ is the relative anion exclusion volume. The exclusion volume-per-unit mass of soil can also be estimated as:

$$V_{ex} = \int (1 - c/C_o) dV$$

[6.25]

where V_{ex} is the exclusion volume (L^3 M^{-1}), c is the local concentration of the anion (M L^{-3}) and C_o its bulk concentration (M L^{-3}), and V is the entire volume encompassing the liquid phase. Instead of using $R < 1$, anion transport may be modeled with a model, with $R = 1$, which restricts the accessible liquid volume (Krupp et al., 1972).

Anions are also adsorbed by the soil through surface complexation and adsorption onto positively charged areas of the solid matrix (Section B, Chapter 7). If the effect of adsorption exceeds exclusion, the anion will be retarded. The retardation factor should be viewed as an effective parameter since it quantifies a variety of adsorption and exclusion processes to which the solute (anion) is subjected.

Breakthrough curves typical for the transport of an excluded anion (Cl$^-$) a nonreactive solute (tritiated water, ^{3}H$_2$O), and an adsorbed cation (Ca^{2+}) are presented in Fig. 6.5. The first two tracers pertain to transport through 30 cm columns containing disturbed Glendale clay loam soil (P. J.
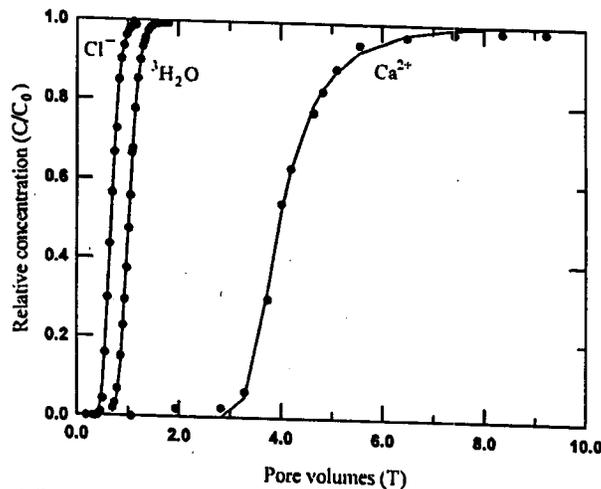

Fig. 6.5 Observed and fitted ADE breakthrough curves for three tracers typifying the transport of anions (Cl$^-$), a (nearly) nonreactive solute (^{3}H$_2$O), and an adsorbing solute (Ca^{2+})

Wierenga, personal communication; van Genuchten and Cleary, 1982), while the Ca^{2+} data are for transport through a 30-cm long column containing a Troup loam and a Savannah fine loam (Leij and Dane, 1989). Analysis of the three breakthrough curves in terms of the ADE, using inverse procedures (Parker and van Genuchten, 1984b), yielded R values of 0.681, 1.027, and 4.120 for Cl^-, ^3H_2O, and Ca^{2+}. Hence, the Cl^- curve was strongly affected by anion exclusion, while ^3H_2O transport was subject to very minor adsorption/exchange.

6.2.3.2 Nonlinear Adsorption

In many cases adsorption, and hence, the retardation factor, cannot be described using a simple K_d approach. For nonlinear equilibrium adsorption, R is given as:

$$R(C) = 1 + \frac{\rho_b}{\theta} \frac{\partial \Gamma}{\partial C}$$

[6.26]

Two common nonlinear adsorption isotherms are the Langmuir and Freundlich equation

$$\Gamma = \frac{k_1 C}{1 + k_2 C} \qquad \text{Langmuir}$$

[6.27]

$$\Gamma = k_3 C^n \qquad \text{Freundlich}$$

[6.28]

where k_1, k_2, k_3, and n are empirical constants. Many other equations for adsorption exist, including some that account for differences between adsorption and desorption isotherms (van Genuchten and Sudicky, 1999).
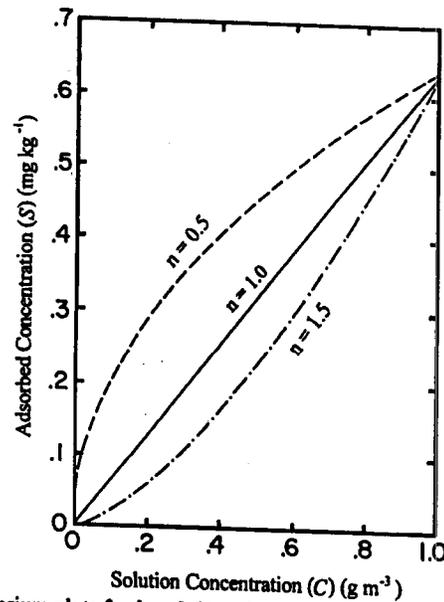

Fig. 6.6 Freundlich equilibrium plots for $k_3 = 0.64$ and three values of the exponent n

The Freundlich isotherm will be used in the following to illustrate the effects of nonlinear equilibrium adsorption on solute transport. In order to keep the calculations simple, the value of k_3 in Equation [6.28] is taken to be 0.64. Three different values of the exponent n are used, viz., 0.5, 1.0, and 1.5, to demonstrate favorable, linear, and unfavorable adsorption isotherms (Fig. 6.6). Calculated distributions of the solution (C) and adsorbed (S) concentrations versus soil depth (z) eight days after application of a 4-day long solute pulse to the soil surface are shown in Fig. 6.7. The same pore water velocity is used as for the example illustrated in Fig. 6.5, but with a smaller dispersion coefficient of D = 25 cm^2 d^{-1} (α_L = 1 cm). Notice that, as in Fig. 6.5, the solution concentration distribution for $n = 1$ (linear adsorption) has a nearly symmetrical shape versus depth. The other two n values yield nonsymmetric profiles.

If $n = 0.5$, a very sharp concentration front develops, while the curve near the soil surface becomes more dispersed. The sharp front can be explained by considering the retardation factor (R) for nonlinear adsorption (Equation [6.26]), which for $n = 0.5, \rho_b = 1.25$ g cm^{-3}, $\theta = 0.40$, and $k_3 = 0.64$ leads to $R = 1+1/C$. This shows that R increases rapidly when C decreases with the extreme $R \rightarrow \infty$, if $C = 0$. Consequently, the apparent solute velocity $v_a = v/R$ is very small at the lower liquid concentrations, but increases at higher values. Of course, higher concentrations cannot move faster than lower concentrations; front sharpening will lead to a steep solute front. This front never becomes a step function because the large concentration gradient across the front will create a large diffusion/ dispersion flux. When $n < 1$, an estimate of the front can be obtained from the average slope of the isotherm between the initial and the maximum concentration. Because in the present example these are zero and approximately one, the average slope of the isotherm is exactly the same as the linear distribution coefficient (dΓ/dC = 0.64). Substituting this value into Equation [6.26] yields $R = 3$. Hence, the apparent solute velocity (v_a) equals 25/3 or 8.33 cm d^{-1}, and the solute front after 8 days is located at a depth of about 67 cm (Fig. 6.7). Transport of favorably adsorbed solutes is frequently modeled with traveling wave solutions (van der Zee, 1990; Simon et al., 1997).

A reverse scenario occurs if $n > 1$ (unfavorable exchange). Adsorption at the lower concentrations is now relatively small and, as displayed in Fig. 6.7, the toe of the front moves through the profile at a
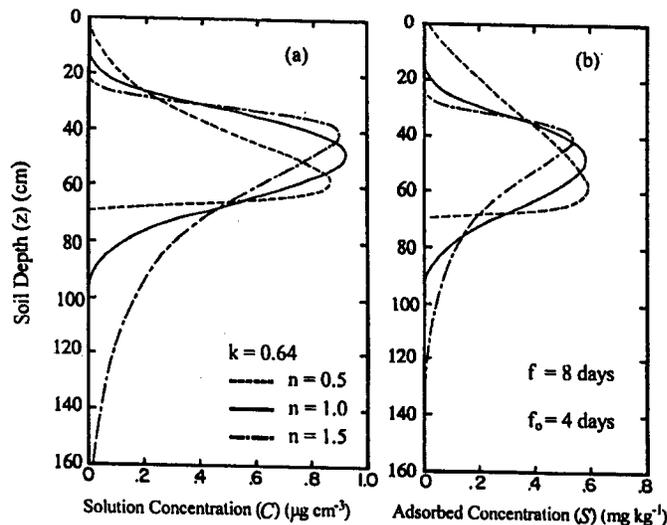

Fig. 6.7   Effect of nonlinear adsorption on solution (C) and adsorbed (S) concentrations in a deep homogeneous soil profile during steady-state flow. The distributions were obtained for the three isotherms shown in Fig. 6.6.

velocity nearly equal to that of an inert solute. Adsorption at the higher concentrations, on the other hand, is much more extensive, resulting in a lower apparent solute velocity in the higher range of concentrations. As a result, the concentration front becomes increasingly dispersed over time. Ignoring dispersion, the velocity of the solute front ($v_a = v/R$) at any given value of C is given by:

$$v_a = \frac{v}{1+3\sqrt{C}}$$ [6.29]

while the depth of the solute front can be approximated by:

$$z(C,t) = z(C,0) + v_a t$$ [6.30]

where $z(C,0)$ is the location of a solute concentration with value C at $t = 0$.

The above discussion pertained to adsorption of a single ion species. Cation exchange processes in transport studies involve at least two species. The simplest case arises when two cations of the same valency and total concentration such as Ca^{2+} and Mg^{2+} are considered. The resulting exchange process is then approximately linear for relatively small changes in the composition of the soil solution. Exchange between Na^+ and Ca^{2+}, on the other hand, is considerably more nonlinear. Equations that quantify the exchange reaction have been proposed by Gapon, Kerr, Vanselow, Eriksson, and others (Section B, Chapter 7).

6.2.4 Nonequilibrium Transport

Solute breakthrough curves for aggregated soils will exhibit asymmetrical distributions or nonsigmoidal concentration fronts. The concept behind physical nonequilibrium models is that differences between regions of the liquid phase lead to mostly lateral gradients in the solute concentration resulting in a diffusive type of solute transfer process. Depending upon the exact pore structure of the medium, asymmetry is sometimes enhanced by desaturation when the relative fraction of water residing in the marginally continuous immobile region increases.

Since most of the sorption sites are only accessible after diffusion through the immobile region of the liquid phase, a corresponding delay in adsorption will occur. The delayed adsorption can also be explained with a kinetic description of the adsorption process. Both cases may be described with chemical nonequilibrium models, which distinguish between sites with equilibrium and kinetic sorption.

Bi-continuum or dual-porosity nonequilibrium models are the most widely used. Only two concentrations need to be considered and the equilibrium ADE (Equation [6.18]) can be readily modified for this purpose. The same dimensionless mathematical formulation can be used for physical and chemical nonequilibrium models. If necessary, the ADE can be modified to incorporate additional nonequilibrium processes and continua.

6.2.4.1 Physical Nonequilibrium

Consider one-dimensional solute movement in an isotropic soil with uniform flow and transport properties during steady flow, and assume that the solute is subject to linear retardation, that is, equilibrium sorption can be described with a linear exchange isotherm. The physical nonequilibrium approach is based on a partitioning of the liquid phase into a mobile or flowing region and an immobile or stagnant region. Solute movement in the mobile region occurs by both advection and dispersion,

whereas solute exchange between the two regions occurs by first order diffusion (Coats and Smith, 1964). Following van Genuchten and Wierenga (1976), the governing equations for the two region model are

$$(\theta_m + f\rho_b K_d)\frac{\partial C_m}{\partial t} = \theta_m D_m \frac{\partial^2 C_m}{\partial x^2} - \theta_m v_m \frac{\partial C_m}{\partial x} - \alpha(C_m - C_{im})$$ [6.31]

$$[\theta_m + (1-f)\rho_b K_d]\frac{\partial C_{im}}{\partial t} = \alpha(C_m - C_{im})$$ [6.32]

where f represents the fraction of sorption sites in equilibrium with the fluid of the mobile region, α is first order mass transfer coefficient (T^{-1}), and the subscripts m and im, respectively, refer to the mobile and immobile liquid regions (with $\theta = \theta_m + \theta_{im}$), while ρ_b and K_d are the soil bulk density and distribution coefficient for linear sorption. Transport Equation [6.31] follows directly from addition of a source/sink term (R_s) to Equation [6.18].

Anion exclusion can be viewed as a particular example of physical nonequilibrium, the exclusion volume roughly corresponds to the immobile region (Krupp et al., 1972). The physical nonequilibrium concept may, therefore, be adapted to describe transport of excluded anions (van Genuchten, 1981) instead of using a retardation factor of less than one.

6.2.4.2 Chemical Nonequilibrium

Sorption of solute, especially for organic chemicals, has often been described with a combined equilibrium and kinetic sorption expression so as to better simulate transport in soils with a wide variety of soil constituents (clay minerals, organic matter, and oxides). The lack of an instantaneous equilibrium for the sorption process is sometimes referred to as chemical nonequilibrium. This terminology is somewhat misleading since the rate of adsorption or exchange is usually determined mostly by physical phenomena such as diffusion through the liquid film around soil particles and inside the aggregates (Boyd et al., 1947; Sparks, 1989).

The simplest and by far most popular approach distinguishes between type-1 sites, with instantaneous adsorption, and type-2 sites, where adsorption obeys a kinetic rate law (Selim et al., 1976). In the case of first-order kinetics, the general adsorption rates can be given with a model similar to Equations [6.19] and [6.20] as:

$$\frac{\partial S_1}{\partial t} = \alpha_1[\Gamma_1(C) - S_1]$$ [6.33]

$$\frac{\partial S_2}{\partial t} = \alpha_2[\Gamma_2(C) - S_2]$$ [6.34]

where α is again a rate constant (T^{-1}), S is the actual adsorbed concentration (M M^{-1}), Γ is the final adsorbed concentration at equilibrium as prescribed by the adsorption isotherm, the subscripts 1 and 2 refer to the type of adsorption site, and $\Gamma_1 + \Gamma_2 = \Gamma$. Because type-1 sites are always at equilibrium, $S_1 = \Gamma_1$ and Equation [6.33] can further be ignored. The transport equation becomes:

$$\frac{\partial C}{\partial t} + \frac{\rho_b}{\theta}\frac{\partial \Gamma}{\partial t} + \frac{\alpha_2 \rho_b}{\theta}(\Gamma_2 - S_2) = D\frac{\partial^2 C}{\partial x^2} - v\frac{\partial C}{\partial x}$$ [6.35]

If the fraction of exchange sites that is at equilibrium (type-1) equals f, and if equilibrium adsorption is governed by the same linear isotherm for both types 1 and 2 ($\Gamma_1 = \Gamma_2$) then:

$$\Gamma_1 + \Gamma_2 = fK_d C + (1-f)K_d C$$ [6.36]

Of course, nonlinear equilibrium isotherms may also be used in nonequilibrium transport models. The complete transport problem can now be written as:

$$\left(1 + \frac{\rho_b f K_d}{\theta}\right)\frac{\partial C}{\partial t} = D\frac{\partial^2 C}{\partial x^2} - v\frac{\partial C}{\partial x} - \frac{\alpha \rho_b}{\theta}\left[(1-f)K_d C - S_2\right]$$ [6.37]

$$\frac{\partial S_2}{\partial t} = \alpha\left[(1-f)K_d C - S_2\right]$$ [6.38]

where the subscript for α has been dropped. This two-site chemical nonequilibrium model reduces to a one-site kinetic nonequilibrium model by setting $f = 0$. The two-site chemical nonequilibrium model was applied successfully to describe solute breakthrough curves by Selim et al. (1976), van Genuchten (1981), and Nkedi-Kizza et al. (1983), among others.

6.2.4.3 General Nonequilibrium Formulation

The two-site and the two-region nonequilibrium models can be cast in the same (dimensionless) model according to Nkedi-Kizza et al. (1984):

$$\beta R \frac{\partial C_1}{\partial T} = \frac{1}{P}\frac{\partial^2 C_1}{\partial X^2} - \frac{\partial C_1}{\partial X} + \omega(C_2 - C_1)$$ [6.39]

$$(1-\beta)R\frac{\partial C_2}{\partial T} = \omega(C_1 - C_2)$$ [6.40]

where β is a partition coefficient, R is a retardation factor, C_1 and C_2 are dimensionless equilibrium and nonequilibrium concentrations, T is time, X is distance, P is the Peclet number, ω is a mass transfer coefficient, and the subscripts 1 and 2 refer to the equilibrium and nonequilibrium phases, respectively. The common dimensionless parameters are defined using an arbitrary characteristic concentration (C_o) and length (L):

$$T = vt/L \quad , \quad X = x/L \quad , \quad P = vL/D \quad , \quad R = 1 + \rho_b K_d/\theta$$ [6.41]

For the physical nonequilibrium model, the remaining dimensionless parameters are

$$\beta = \frac{\theta_m + f \rho_b K_d}{\theta + \rho_b K_d} \quad , \quad \omega = \frac{\alpha L}{\theta v} \quad , \quad C_1 = \frac{C_m}{C_o} \quad , \quad C_2 = \frac{C_{im}}{C_o} \qquad [6.42]$$

whereas for the chemical nonequilibrium model:

$$\beta = \frac{\theta_m + f \rho_b K_d}{\theta + \rho K_d} \quad , \quad \omega = \frac{\alpha(1-\beta)RL}{v} \quad , \quad C_1 = \frac{C}{C_o} \quad , \quad C_2 = \frac{S_2}{(1-f)K_d C_o} \qquad [6.43]$$

In the chemical engineering literature, $\alpha L/v$ is known as the Damköhler number; it quantifies the rate of the reaction or exchange relative to advective transport.

6.3 Solutions of the Advection-Dispersion Equation

The research and management of solute behavior in soils almost invariably require that the temporal and spatial solute distribution be known. Solute distributions as a function of time and/or space can be estimated with a variety of analytical and numerical solutions of the ADE, some of which will be briefly reviewed in the following.

6.3.1 Basic Concepts

A complete mathematical formulation of the transport problem requires that the pertinent dependent variable or concentration type is used and that the proper auxiliary conditions are specified.

6.3.1.1 Concentration Types

Concentration is conventionally defined as the amount of solute-per-unit volume of the liquid. Since microscopic concentrations are based on a relatively small scale, a concentration at a larger scale needs to be introduced to allow use of the ADE which is based on larger macroscopic variables and parameters. For this purpose, a macroscopic resident or volume-averaged concentration (C_R) is defined as:

$$C_R = \frac{1}{\Delta V} \iiint c \, dV \qquad [6.44]$$

where c is the variable local-scale (microscopic) concentration ($M\,L^{-3}$) in a volume element (V) and V is some representative elementary volume (Bear and Verruijt, 1987).

A different concentration type may be encountered at soil boundaries. In many solute displacement experiments, the concentration is determined from effluent samples as the ratio of the solute flux (J_s) and water flux (J_w) densities:

$$C_F = J_s / J_w \qquad [6.45]$$

where C_F is the flux averaged concentration. This concentration represents the mass of solute-per-unit volume of fluid passing through a soil cross-section during an elementary time interval (Kreft and Zuber, 1978). For a one-dimensional solute flux consisting of an advective and a dispersive component, the flux-averaged concentration can be derived from the resident concentration according to the transformation:

$$C_F = C_R - \frac{D}{v}\frac{\partial C_R}{\partial x}$$

[6.46]

The resident concentration may be determined from the flux averaged concentration using (van Genuchten et al., 1984):

$$C_R(x,t) = \frac{v}{D}\exp\left(\frac{vx}{D}\right)\int_x^\infty \exp\left(-\frac{v\xi}{D}\right)C_F(\xi,t)d\xi$$

[6.47]

Additional transformations between flux and resident type concentrations are given by Parker and van Genuchten (1984a).

The difference between C_R and C_F is usually small, except when the second term on the right-hand side of Equation [6.46] is relatively large. It should be noted that a distinction between flux and resident type can be made for both the application and the detection of solutes (Kreft and Zuber, 1978, 1986). In soil science, a flux type application mode is often implicitly assumed (Parker and van Genuchten, 1984a). Flux-averaged concentrations are typically used when it is not possible to determine or specify a reliable value for the (resident) concentration. Resident concentrations are used for solute detection with, for example, time domain reflectometry, and to specify most initial conditions. Flux-averaged concentrations, on the other hand, are used for effluent samples, and to specify the influent concentration in most boundary value problems. Unless stated otherwise, it is assumed that solute concentrations are of the resident type.

Averaged concentrations can also be defined in terms of the observation scale, the latter exceeding the macroscopic scale associated with using the ADE. A time-averaged concentration (C_T), is obtained by averaging over a time interval (Δt) about a discrete time (t_o) (Fischer et al., 1979):

$$C_T(x,t_o) = \frac{1}{\Delta t}\int_{t_o-\Delta t/2}^{t_o+\Delta t/2} C(x,t)dt$$

[6.48]

where C is a continuous solution of the solute concentration, which can be obtained by solving the ADE. This type of concentration occurs if solute breakthrough curves are measured using, for example, fraction collectors or gamma ray attenuation. Similarly, a one-dimensional spatial average can be defined as:

$$C_L(x_o,t) = \frac{1}{\Delta x}\int_{x_o-\Delta x/2}^{x_o+\Delta x/2} C(x,t)dx$$

[6.49]

This concentration may be used to describe experimental results obtained for samples with centroid (x_o) and length (Δx). This situation occurs, for example, when the measured concentration of a large core sample is to be modeled as a point value (Leij and Toride, 1995).

6.3.1.2 Boundary and Initial Conditions

Initial and boundary conditions need to be specified in order to obtain a meaningful solution of the ADE. For a finite or semi-infinite soil, the initial condition can be formulated as:

$$C(x,0) = f(x) \qquad x \geq 0 \tag{6.50}$$

where $f(x)$ is an arbitrary function. Initial concentrations are almost invariably of the resident type.

The selection of the most appropriate boundary conditions for a transport problem is a somewhat esoteric topic that has received considerable attention in the literature. This is partly due to a lack of detailed experimental information for evaluating and applying boundary conditions, and inherent shortcomings of the transport equation itself at boundaries.

Many transport problems involve the application to the soil of a solute, whose influent concentration may be described by a function $g(t)$. The application method may be pumping, ponding, or sprinkling. Two different types of inlet conditions are used, which assume either continuity in solute concentration or solute flux density. Simultaneous use of both conditions is seldom possible. It is generally more desirable to ensure mass conservation in the whole system than a continuous concentration at the inlet. The solute fluxes at the inlet boundary are, therefore, equated to obtain the following third or flux type inlet condition:

$$\left(vC - D\frac{\partial D}{\partial x} \right)_{x=0^+} = vg(t) \tag{6.51}$$

where 0^+ indicates a position just inside the soil. It is assumed that there is no dispersion outside the soil. The alternative condition requires the concentration to be continuous across the interface at all times. At smaller scales, such continuity will likely exist. However, at the scale of the ADE, it appears difficult to maintain a constant concentration at the interface, particularly during the initial stages of solute displacement for low influent fluxes and high dispersive fluxes in the soil. Mathematically, the first or concentration type condition is expressed as:

$$C(0,t) = g(t) \qquad t > 0 \tag{6.52}$$

The outlet condition can be defined as a zero gradient at a finite or infinite distance from the inlet. The infinite outlet condition,

$$\frac{\partial C}{\partial x}(\infty, t) = 0 \tag{6.53}$$

is more convenient for mathematical solutions than the finite condition,

$$\frac{\partial C}{\partial x}\left(L^-, t\right) = 0 \tag{6.54}$$

The use of Equation [6.53] implies that there is a semi-infinite fictitious soil layer beyond $x = L$, with identical properties as the actual soil. Such a layer does not affect the movement of the solute in the actual soil upstream of the exit boundary. Since the transport at the outlet cannot be precisely described, the intuitive contradiction of an infinite mathematical condition to describe a finite physical system is often more acceptable than using Equation [6.54], which precludes dispersion inside the soil near the outlet.

The formulation of the boundary and inlet conditions should account for the injection and detection modes in order to arrive at a mathematically consistent formulation of the problem with the same concentration type as independent variable. Only differences in detection mode for finite and semi-infinite systems will here be explored. The ADE in terms of the (usual) resident concentration is given as:

$$\frac{\partial C_R}{\partial t} = D \frac{\partial^2 C_R}{\partial x^2} - v \frac{\partial C_R}{\partial x}$$

[6.55]

subject to a uniform initial condition, a third-type inlet condition, and a finite or infinite outlet condition:

$$C_R(x,0) = C_i$$

[6.56]

$$\left(v C_R - D \frac{\partial C_R}{\partial x} \right)_{x=0^+} = v g(t)$$

[6.57]

$$\frac{\partial C_R}{\partial x}(\infty, t) = 0 \quad \text{or} \quad \frac{\partial C_R}{\partial x}(L, t) = 0$$

[6.58]

This problem can be written in terms of a flux-averaged concentration using Equation [6.48] according to (Parker and van Genuchten, 1984b):

$$\frac{\partial C_F}{\partial t} = D \frac{\partial^2 C_F}{\partial x^2} - v \frac{\partial C_F}{\partial x}$$

[6.59]

subject to

$$C_F(x,0) = C_i$$

[6.60]

$$C_F(0,t) = g(t)$$

[6.61]

$$\frac{\partial C_F}{\partial x}(\infty, t) = 0 \quad \text{or} \quad \frac{\partial C_F}{\partial x}(L, t) = -\frac{D}{v} \frac{\partial^2 C_R}{\partial x^2}(L, t)$$

[6.62]

Notice that the mathematical problem for the flux mode involves a simpler first-type inlet condition with mass being conserved, unlike the use of a first-type condition for a resident concentration. The solution for C_R for a semi-infinite system involving a first-type inlet condition is the same as the solution for C_F that conserves mass. As shown by Toride et al. (1994), the transformation is less

convenient for nonuniform initial conditions or finite systems. Solutions for C_F are then more easily obtained by transforming C_R according to Equation [6.46].

Differences between the preferred third type solution for C_R and its first type solution are usually small except for low values of the dimensionless time [$\varsigma = v^2 t/(RD)$] (van Genuchten and Parker, 1984). The relative mass balance error in a semi-infinite soil profile if a first type rather than a third-type inlet condition is used, is given in Fig. 6.8 (van Genuchten and Parker, 1984). The error pertains to the transport of a tracer solution of concentration (C_o) into an initially solute-free semi-infinite soil profile. Especially for small ς, a substantial error may occur. Unless stated otherwise, a resident concentration is used in conjunction with a third-type inlet condition.

6.3.2 Analytical Solutions

Analytical solutions can formally be obtained only for linear transport problems. It would appear that analytical solutions are not very useful for transport in field soils where there is (1) spatial and temporal variability of flow and transport parameters, (2) transient flow, especially for unsaturated soils, and (3) nonuniformity in the boundary and initial conditions. However, analytical solutions can still be quite valuable. A nonlinear transport problem may be linearized through a suitable transformation to obtain a problem for which an analytical solution is available. Also, analytical solutions provide quick estimates of solute behavior over large temporal and spatial scales while they may offer insight into the underlying transport processes. Moreover, there is usually a lack of input parameters for field problems, which diminishes the advantage of numerical over analytical model results. Analytical solutions are also routinely used to evaluate the performance of numerical schemes. Finally, the mathematical and physical conditions tend to be well defined for laboratory settings and an analytical solution can often be used, especially to estimate transport parameters by fitting analytical solutions to experimental data (Parker and van Genuchten, 1984; van Genuchten and Parker, 1987).

6.3.2.1 Variable Transformation

One straightforward way to obtain an analytical solution is to transform the ADE to an equation for which a solution already exists. As an example, consider transport in an infinite system given by:

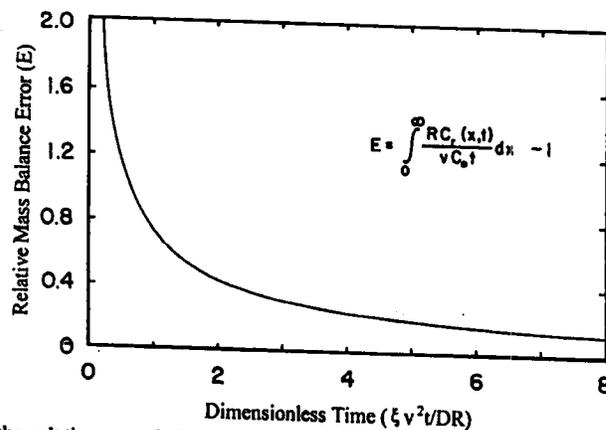$$E = \int_0^\infty \frac{R C_r(x,t)}{v C_o t} dx - 1$$

Fig. 6.8   Plot of the relative mass balance error versus dimensionless time for a semi-infinite profile when a first-type rather than a third-type inlet condition is used [After van Genuchten and Parker, 1984]

$$R\frac{\partial C}{\partial t} = D\frac{\partial^2 C}{\partial x^2} - v\frac{\partial C}{\partial x}$$

[6.63]

$$C(x,0) = \begin{cases} C_o & x < 0 \\ 0 & x > 0 \end{cases}$$

[6.64]

The new coordinates

$$\xi = x - vt$$
$$\tau = t$$

[6.65]

transform the ADE into a heat or solute diffusion problem given by:

$$R\frac{\partial C}{\partial \tau} = D\frac{\partial^2 C}{\partial \xi^2}$$

[6.66]

$$C(\xi,0) = \begin{cases} C_0 & \xi < 0 \\ 0 & \xi > 0 \end{cases}$$

[6.67]

The solution for this problem can be readily found in the literature on diffusion problems (Carslaw and Jaeger, 1959; Crank, 1975):

$$C(x,t) = \frac{C_o}{2}\text{erfc}\left(\frac{Rx - vt}{\sqrt{4RDt}}\right)$$

[6.68]

Other transformations to the diffusion problem have been employed as well (Brenner, 1962; Selim and Mansell, 1976; Zwillinger, 1989). Transformation of time to a time-integrated flow variable sometimes also allows one to derive an analytical solution of the nonlinear ADE for transient flow (Wierenga, 1977; Parker and van Genuchten, 1984b; Huang and van Genuchten, 1995).

6.3.2.2 Laplace Transformation

The ADE is commonly solved directly with the method of Laplace transforms. The solution procedure will be illustrated here for an initially solute-free semi-infinite soil with a constant solute flux (vC_o) or concentration (C_o) at the inlet boundary. The mathematical problem consists of solving the ADE given by Equation [6.63] subject to:

$$C - \delta\frac{D}{v}\frac{\partial D}{\partial x} = C_o \qquad \delta = \begin{cases} 0 & \text{first type} \\ 1 & \text{third type} \end{cases}$$

[6.69]

$$\frac{\partial C}{\partial x}(\infty, t) = 0 \tag{6.70}$$

with δ as a coefficient depending on the type of inlet condition. The Laplace transform ($\mathscr{L}$) of the solute concentration with respect to time is defined as (Spiegel, 1965):

$$\overline{C}(x, s) = \mathscr{L}[C(x,t)] = \int_0^\infty C(x, t) \exp(-st) dt \tag{6.71}$$

where s is the (complex) transformation variable (T^{-1}). This transformation changes the transport equation from a partial to an ordinary differential equation:

$$\frac{d_2 \overline{C}}{dx^2} - \frac{v}{D}\frac{d\overline{C}}{dx} - \frac{sR}{D}\overline{C} = 0 \tag{6.72}$$

subject to

$$\overline{C} - \delta \frac{D}{v}\frac{d\overline{C}}{dx} = \frac{C_o}{s} \tag{6.73}$$

$$\frac{d\overline{C}}{dx}(\infty, s) = 0 \tag{6.74}$$

where the bar denotes a transformed variable. The following solution for the concentration in the Laplace domain is obtained with help of the inlet condition:

$$\overline{C}(x, s) = \frac{v}{v - \delta \lambda^- D}\frac{C_o}{s}\exp(\lambda^- x) \quad , \quad \lambda^- = \frac{v}{2D} - \left[\left(\frac{v}{2D}\right)^2 + \frac{SR}{D}\right]^{1/2} \tag{6.75}$$

Inversion of this solution may be done with a table of Laplace transforms, by applying the inversion theorem, or by using a numerical inversion program. It should be noted that the solution for a finite outlet condition is also possible with the Laplace transform, although a bit more cumbersome (Brenner, 1962; Leij and van Genuchten, 1995).

6.3.2.3 Equilibrium Transport

Van Genuchten and Alves (1982) provided a compendium of available analytical one-dimensional solutions for a variety of mathematical conditions and physical processes. Four common analytical solutions for a zero initial condition involving a first- or third-type inlet condition and an infinite or finite outlet condition are listed in Table 6.2. The solutions may be expressed in terms of the dimensionless variables (P), (T), and (X) (Equation [6.41]). Typically, L is equal to the position of the outlet (the column length) for a finite system, whereas for a semi-infinite soil system, L can be assigned to any arbitrary length.

Fig. 6.9 contains solute profiles, $[C/C_o(X)]$ according to the solutions listed in Table 6.2 using $R = 1$ and two different values for P and T for a first- (A1) or a third-type (A2) inlet condition assuming an infinite outlet condition, or a first- (A3) or third-type (A4) inlet condition in case of finite outlet condition. The predicted profile for a first-type condition (A1, A3) for the lower Peclet number ($P = 5$) lies considerably above the line predicted for a third-type condition (A2, A4). The effect of the outlet condition is initially minor, but when the solute front reaches the outlet (L), a clear difference between a finite and an infinite outlet condition can be observed for both a first (A1, A3) and a third-type (A2, A4) inlet condition. The simpler solution for a semi-infinite system can, in many cases, be used to approximate the solution for a finite condition; van Genuchten and Alves (1982) formulated the empirical restriction:

$$X < 0.9 - 8 / P \qquad\qquad [6.76]$$

on the position for which such an approximation is reasonable. For smaller times ($T < 1$), when the solute has not reached the outlet, the finite and infinite outlet condition obviously lead to a similar solution.

Table 6.2 Analytical solutions of the ADE for different boundary conditions after van Genuchten and Alves (1982)

Case	Inlet Condition	Exit Condition	Analytical Solution $C(x,t)$
A1	$C(0,t) = C_o$	$\dfrac{\partial C}{\partial x}(\infty,t) = 0$	$\dfrac{1}{2}\operatorname{erfc}\left(\dfrac{Rx - vt}{(4RDt)^{1/2}}\right) + \dfrac{1}{2}\exp\left(\dfrac{vx}{D}\right)\operatorname{erfc}\left(\dfrac{Rx + vt}{(4RDt)^{1/2}}\right)$
A2	$\left(vC - D\dfrac{\partial C}{\partial x}\right)_{x=0} = vC_o$	$\dfrac{\partial C}{\partial x}(\infty,t) = 0$	$\dfrac{1}{2}\operatorname{erfc}\left(\dfrac{Rx - vt}{(4RDt)^{1/2}}\right) - \dfrac{1}{2}\left(1 + \dfrac{vx}{D} + \dfrac{v^2 t}{DR}\right)\operatorname{erfc}\left(\dfrac{Rx + vt}{(4RDt)^{1/2}}\right)$ $+\left(\dfrac{v^2 t}{\pi RD}\right)^{1/2}\exp\left(\dfrac{(Rx - vt)^2}{4RDt}\right)$
A3	$C(0,t) = C_o$	$\dfrac{\partial C}{\partial x}(L,t) = 0$	$1 - \displaystyle\sum_{m=1}^{\infty}\dfrac{2\beta_m \sin\left(\dfrac{\beta_m x}{L}\right)\exp\left(\dfrac{vx}{2D} - \dfrac{v^2 t}{4DR} - \dfrac{\beta_m^2 Dt}{L^2 R}\right)}{\beta_m^2 + \left(\dfrac{vL}{2D}\right)^2 + \dfrac{vL}{2D}}$ $\beta_m \cot(\beta_m) + \dfrac{vL}{2D} = 0$
A4	$\left(vC - D\dfrac{\partial C}{\partial x}\right)_{x=0} = vC_o$	$\dfrac{\partial C}{\partial x}(L,t) = 0$	$1 - \displaystyle\sum_{m=1}^{\infty}\dfrac{\dfrac{2vL}{D}\beta_m\left[\beta_m\cos\left(\dfrac{\beta_m x}{L}\right) + \dfrac{vL}{2D}\sin\left(\dfrac{\beta_m x}{L}\right)\right]\exp\left(\dfrac{vx}{2D} - \dfrac{v^2 t}{4DR} - \dfrac{\beta_m^2 Dt}{L^2 R}\right)}{\left[\beta_m^2 + \left(\dfrac{vL}{2D}\right)^2 + \dfrac{vL}{2D}\right]\left[\beta_m^2 + \left(\dfrac{vL}{2D}\right)^2\right]}$ $\beta_m \cot(\beta_m) - \dfrac{\beta_m^2 D}{vL} + \dfrac{vL}{2D} = 0$

For a third-type inlet condition, the concentration at $X \doteq 0$ just inside the soil is not equal to the influent concentration, even at time $T = 1$. Although the jump in concentration is physically odd, mass conservation is ensured. For the higher Peclet number ($P = 20$), deviations between a first- and a third-type inlet condition are significantly reduced. This is in accordance with Fig. 6.8, which shows a smaller error for increased $v^2 t / RD$.

Large differences in the predicted concentration may occur if the solute front approaches the outlet at $X = 1$ or $x = L$. Calculated concentrations according to solutions A1, A2, A3, and A4 versus the Peclet number at the outlet for $T = 1$ are illustrated in Fig. 6.10. The greatest difference occurs for small Peclet numbers, namely, when hydrodynamic dispersion is relatively important. The nature of hydrodynamic dispersion suggests that C/C_o should be approximately 0.5 for $X = T = R = 1$, the average of the zero initial concentration and the influent concentration (C_o). Because of the effect of the boundary conditions, this only happens when the Peclet number exceeds 10 or more, depending on the type of solution. For the first-type inlet condition (A1, A3), C/C_o exceeds 0.5 at low Peclet numbers since a considerable amount of solute is forced to diffuse into the column to establish a constant inlet concentration.

Differences between calculated solute breakthrough curves because of boundary conditions are further depicted in Fig. 6.11 for three different Peclet numbers. Notice that for $P = 60$, the curves are almost indistinguishable, considering the margin of error of most solute displacement experiments. The results in Fig. 6.11 show that the choice of inlet and outlet conditions for determining parameters from breakthrough experiments becomes less important when P exceeds about 30.

Finally, for displacement experiments involving finite columns, it may be of interest to quantify the amount of solute that can be stored in the liquid and sorbed phases of the soil (Equation [6.24]). When, beginning at $t = 0$, a solution with concentration (C_o) is applied to a soil column, holdup can be defined as (Nauman and Buffham, 1983):

$$H = \frac{v}{L} \int_0^\infty \frac{C_o - C(L,t)}{C_o} dt$$

[6.77]

This amounts to the integration of the complementary solute concentration versus dimensionless time, namely, the area above the breakthrough curves in Fig. 6.11. Van Genuchten and Parker (1984)
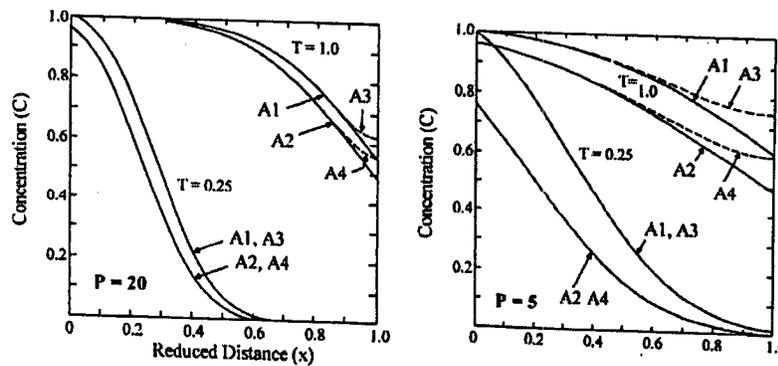

Fig. 6.9 Plot of the concentration (C/C_o) as a function of distance (X) calculated for four different combinations of boundary conditions according to the solutions in Table 6.2 at two different times for a Peclet number of 5 and 20 [After van Genuchten and Alves, 1982]
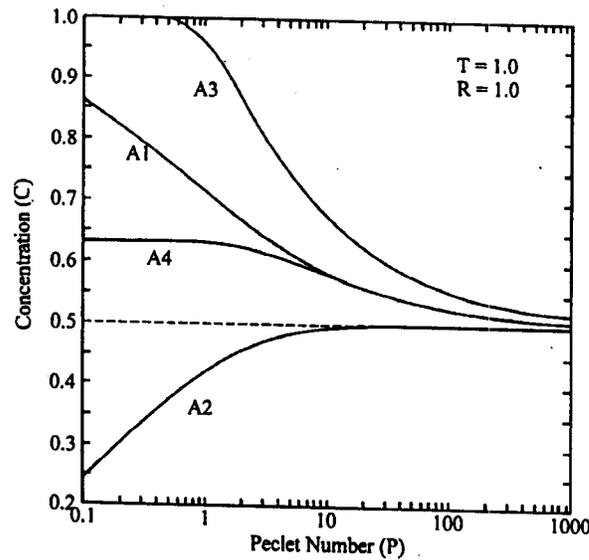
Fig. 6.10 Solute concentration predicted with solutions A1, A2, A3, and A4 as a function of the Peclet number at $T = 1$ and $X = 1$ [After van Genuchten and Alves, 1982]

showed that $H = R$ for solutions A1 and A4, $H = R[1+(1/P)]$ for solution A2 and $H = R\{1 - (1/P)[1 - \exp(-P)]\}$ for solution A3. In case of anion exclusion, the relative exclusion volume equals $1-R$ and the column holdup will be less than one.

6.3.2.4 Nonequilibrium Transport

Analytical solutions for one-dimensional bimodal nonequilibrium transport have been presented by, among others, Lindstrom and Narasimhan (1973), Lindstrom and Stone (1974), Lassey (1988), and Toride et al. (1993). The boundary value problem involving solute application with a constant concentration may be specified by Equations [6.39], [6.40], and [6.53] subject to the following conditions:

$$C_1(X,0) = C_2(X,0) = 0 \tag{6.78}$$

$$\left(C_1 - \frac{1}{P}\frac{\partial C_1}{\partial X}\right)_{X=0^+} = 1 \tag{6.79}$$

$$\frac{\partial C_1}{\partial X}(\infty, T) = 0 \tag{6.80}$$

Solutions for the equilibrium and nonequilibrium concentrations are

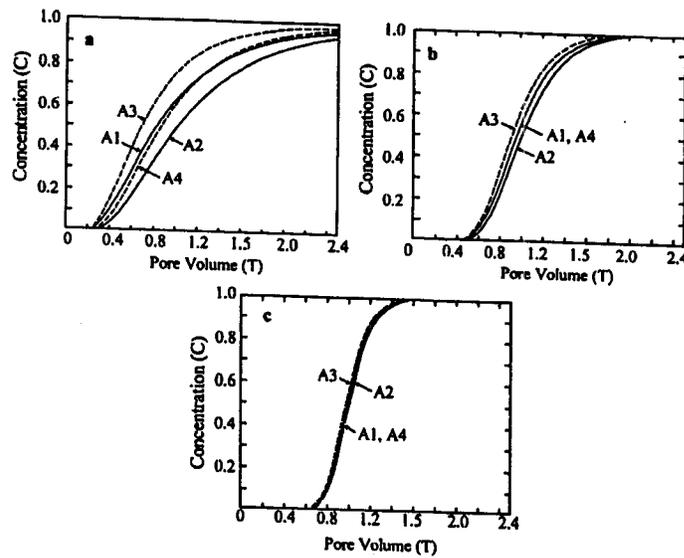$$C_1 = \int_0^T J(a,b)G(X,\tau)d\tau \tag{6.81}$$

Fig. 6.11 Solute breakthrough curves predicted with the four analytical solutions of Table 6.2 for three different Peclet numbers [After van Genuchten and Alves, 1982]

$$C_2 = \int_0^T [1 - J(b,a)] G(X,\tau) d\tau \tag{6.82}$$

where the auxiliary (equilibrium) function $G(X,\tau)$ for resident concentrations is defined as:

$$G(X,\tau) = \sqrt{\frac{P}{\pi\beta R\tau}} \exp\left(-\frac{(\beta RX - \tau)^2}{4\beta R\tau/P}\right) - \frac{P}{2\beta R} \operatorname{erfc}\left[\frac{\beta RX + \tau}{\sqrt{4\beta R\tau/P}}\right] \tag{6.83}$$

and for flux-averaged concentrations by:

$$G(X,\tau) = \sqrt{\frac{\beta RPX^2}{4\pi\tau^3}} \exp\left(-\frac{(\beta RX - \tau)^2}{4\beta R\tau/P}\right) \tag{6.84}$$

Furthermore, J denotes Goldstein's J function (Goldstein, 1953), which is defined as:

$$J(a,b) = 1 - \exp(-b) \int_0^a \exp(-x) I_0\left(2\sqrt{ab}\right) d\xi \tag{6.85}$$

with I_0 as the zero order modified Bessel function. The variables a and b are given by

$$a = \frac{\omega\tau}{\beta R} \quad , \quad b = \frac{\omega(T-\tau)}{(1-\beta)R} \tag{6.86}$$

The above solution for a flux-averaged concentration was used to describe breakthrough data for the pesticide 2,4,5-T (2,4,5-trichlorophenoxyacetic acid) as observed from a 30-cm long soil column containing aggregated (< 6 mm) Glendale clay loam (van Genuchten and Parker, 1987). The nonequilibrium model with three adjustable parameters (P, β, ω) provided an excellent description of the data (Fig. 6.12b). The retardation factor (R) was estimated independently, using the distribution coefficient obtained from batch experiments, according to Equation [6.23]. A one parameter ADE fit (using P as adjustable parameter) did not yield a good description of the data (Fig. 6.12a) while a similar two parameter (P, R) fit, which is not shown, gave results that were only marginally different from those shown in Fig. 6.12a.

As pointed out by van Genuchten and Dalton (1986), the main disadvantage of the first order physical nonequilibrium approach is the obscure dependency of the transfer coefficient (α or ω) on the actual diffusion process in the aggregate, particularly the value for the diffusion coefficient and the aggregate geometry. For well-defined structured or aggregated porous media (media for which the size and geometry of all aggregates are known), the diffusion process inside the aggregate can be modeled, which allows a more detailed description of the concentration inside the aggregate. Analytical solutions are available for several aggregate geometries. The simplified immobile concentration, which is used in the general nonequilibrium formulation, can always be obtained by averaging the more detailed solution over the aggregate volume.

6.3.2.5 Time Moments

Moments are frequently used to characterize statistical distributions such as those of solute particles (concentrations) versus time or positions. Analytical expressions for lower order moments are
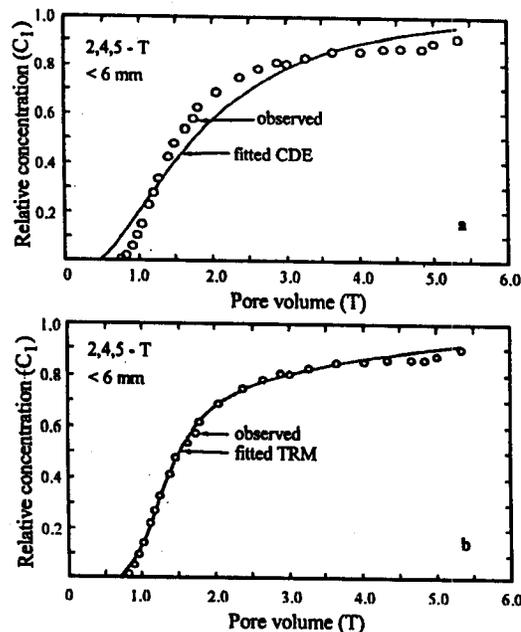

Fig. 6.12 Observed and fitted effluent curves for 2,4,5-T movement through Glendale clay loam. The fitted curves were based on: (a) the equilibrium ADE and (b) the nonequilibrium ADE.

sometimes derived for deterministic transport models, especially when a direct analytical solution may be difficult to obtain. Moment analysis is more widely employed in stochastic than deterministic transport models since the uncertainty in both model parameters and predicted results is most conveniently quantified with moments. Only time moments will here be considered.

The pth (time) moment of the breakthrough curve, as obtained, say, from effluent samples collected from a soil column (with length $x = L$) to which a solute pulse is applied during steady water flow, is defined as:

$$m_p(L) = \int_0^\infty t^p C(L,t)dt \qquad (p = 0,1,2,\ldots)$$

[6.87]

The zero moment is proportional to the total solute mass, the first moment quantifies the mean displacement, the second moment is indicative of the variance (dispersion), whereas the third moment quantifies the asymmetry or skewness of the breakthrough curve. Normalized moments (μ_p) are obtained as follows:

$$\mu_p = \frac{m_p}{m_0}$$

[6.88]

The mean breakthrough time is given by μ_1. Central moments are defined with respect to this mean according to:

$$\mu'_p(L) = \frac{1}{m_0} \int_0^\infty (t - \mu_1)^p C(L,t)dt$$

[6.89]

The variance of a breakthrough curve, which can be used to assess solute dispersion, is given by the second central moment (μ_2'). The degree of asymmetry of the breakthrough curve is indicated by its skewness ($\mu_3'/(\mu_2')^{3/2}$).

The previous definitions are employed to obtain numerical values for moments from experimental results. Substitution of an analytical solution for the solute concentration into the definitions allows the derivation of algebraic expressions for time moments. Values for transport parameters can be obtained by equating numerical and algebraic moments (Leij and Dane, 1992; Jacobsen et al., 1992). This procedure is not reliable if experimental moments of higher order ($p > 2$) are needed since even small deviations, at larger times, between experimental and modeled concentrations will greatly bias such moments.

Algebraic moments are normally obtained by using the solution for the concentration in the Laplace domain. The following equality can be established from properties of the Laplace transform (Spiegel, 1965):

$$m_p(x) = (-1)^p \lim_{s \to 0} \frac{d^p \overline{C}(x,s)}{ds^p}$$

[6.90]

where, as before, $\overline{C}(x,s)$ is the concentration in the Laplace domain, and s is the (complex) transformation variable. Expressions for moments can hence be obtained by differentiating the

solution in the Laplace domain and letting the Laplace variable go to zero (Aris, 1958; van der Laan, 1958). This task is conveniently handled by mathematical software.

Time moments will now be considered for three different transport problems. First, the mathematical problem for physical nonequilibrium transport can be written as:

$$\theta_m R \frac{\partial C_m}{\partial t} + \theta_{im} R \frac{\partial C_{im}}{\partial t} = \theta_m D_m \frac{\partial^2 C_m}{\partial x^2} - \theta v \frac{\partial C_m}{\partial x}$$

[6.91]

$$\theta_{im} R \frac{\partial C_{im}}{\partial t} = \alpha(C_m - C_{im})$$

[6.92]

The conditions for instantaneous solute application to a soil are

$$C(x,0) = 0 \qquad 0 \leq x < \infty$$

[6.93]

$$C(0,t) = \frac{m_0}{v} \delta(t)$$

[6.94]

$$\frac{\partial C}{\partial x}(\infty,t) = 0$$

[6.95]

where m_0 is the solute mass that is applied per unit area of soil solution at $t = 0$, and $\delta(t)$ is the Dirac delta function (T^{-1}). The first-type inlet condition is used to describe flux-averaged concentrations such as effluent samples from column displacement experiments. Second, the equilibrium problem is defined by the same set of equations by setting $\theta_m = \theta$, $\theta_{im} = 0$, and $\alpha \to 0$. Third, the chemical nonequilibrium transport equations are as follows:

$$\frac{\partial C}{\partial t} + \frac{\rho_b}{\theta} \frac{\partial S}{\partial t} = D \frac{\partial^2 C}{\partial x^2} - v \frac{\partial C}{\partial x}$$

[6.96]

$$\frac{\partial S}{\partial t} = \alpha(K_d C - S)$$

[6.97]

These equations are also subject to boundary and initial conditions in Equations [6.93] through [6.95].

Formulas for the mean breakthrough time (μ_1) and the variance (μ_2') of the breakthrough curve predicted for these three models are presented in Table 6.3. The expressions suggest that nonequilibrium conditions do not affect the mean travel time but they do increase solute spreading. Since only the solution in the Laplace domain is needed, moment analysis is particularly useful for more complex transport problems to study the general behavior of the breakthrough curve.

6.3.3 Numerical Solutions

The solution of many practical transport problems requires the use of numerical methods because of changes in water saturation (as the result of irrigation, evaporation, and drainage), spatial and

temporal variability of soil properties, or complicated boundary and initial conditions. Numerical methods are based on a discretization of the spatial and temporal solution domain, and subsequent calculation of the concentration at discrete nodes in the domain. This approach is in contrast with analytical methods, which offer a continuous description of the concentration. In some cases, a combination of analytical and numerical techniques may be employed (Sudicky, 1989; Moridis and Reddell, 1991; Li et al., 1992).

6.3.3.1 Introduction

The accuracy of the numerical results depends on the input parameters, the approximation of the governing partial differential equation, the discretization, and implementation of the numerical solution in a computer code solving the simulated problem. Numerous texts exist on the numerical modeling of flow and transport in porous media (Pinder and Gray, 1977; Huyakorn and Pinder, 1983; Campbell, 1985; van der Heijde et al., 1985; Istok, 1989).

The many numerical methods for solving the ADE can be classified into three groups (Neuman, 1984): (1) Eulerian, (2) Lagrangian, and (3) mixed Lagrangian-Eulerian. In the Eulerian approach, the transport equation is discretized by the method of finite differences or finite elements using a fixed mesh. For the Lagrangian approach, the mesh deforms along with the flow while it is stable in a moving coordinate system. A two-step procedure is followed for a mixed approach. First, advective transport is solved using a Lagrangian approach and concentrations are obtained from particle trajectories. Subsequently, all other processes including sinks and sources are modeled with an Eulerian approach using finite elements, finite differences, etc.

The method of finite differences (Bresler and Hanks, 1969; Bresler, 1973) and the Galerkin method of finite elements (Gray and Pinder, 1976; van Genuchten, 1978) belong to the first group as do the previously mentioned combination of analytical and numerical techniques. The finite difference and finite element methods were the first numerical methods used for solute transport problems and, in spite of their problems discussed below, are still the most often utilized methods. Numerical experiments have shown that both methods give very good results if significant dispersion exists as quantified with the Peclet number. If advection is dominant, however, numerical oscillations may

Table 6.3 Mean breakthrough time (μ_1) and variance (μ_2') for the equilibrium and nonequilibrium solution of the ADE at a distance x from the inlet as a result of a Dirac delta input described with a first-type inlet condition (i.e., flux-averaged concentration).

ADE model	Mean breakthrough time, μ_1	Variance μ_2'
Equilibrium	$\dfrac{Rx}{v}$	$\dfrac{2DR^2x}{v^3}$
Nonequilibrium		
Two-Region	$\dfrac{Rx}{v}$	$\dfrac{2\theta_m D_m R^2 x}{\theta v^3} + \dfrac{2\theta(1-\beta)^2 R^2 x}{\alpha v}$
Two-Site	$\dfrac{Rx}{v}$	$\dfrac{2DR^2x}{v^3} + \dfrac{2(1-\beta)Rx}{\alpha v}$

occur for both methods and small spatial increments should be used. It may not always be possible to decrease the spatial step size due to the associated increase in computations and a variety of approaches have been developed to overcome the oscillations (Chaudhari, 1971; van Genuchten and Gray, 1978; Donea, 1991).

Lagrangian solution methods will result in very few numerical oscillations (Varoglu and Finn, 1982). However, Lagrangian methods, which are based on the method of characteristics, suffer from inherent diffusion and do not conserve mass. They are difficult to implement for two- and three-dimensional problems. Instabilities resulting from inadequate spatial discretization may occur during longer simulations due to deformation of the stream function, especially if the solute is subject to sorption, precipitation, and other reactions.

The mixed approach has been applied by several authors (Konikov and Bredehoeft, 1978; Molz et al., 1986; Yeh, 1990). In view of the different behavior of the diffusive (parabolic) and advective (hyperbolic) terms of the ADE, the problem is decomposed into an advection and a diffusion problem. Advective transport is solved with the Lagrangian approach while all other terms are solved with the Eulerian approach. The trajectories of flowing particles are obtained using continuous forward particle tracking (to follow a set of particles as they move through the flow domain), single-step reverse particle tracking (the initial position of particles arriving at nodal points was calculated for each time step), and a combination of both approaches. Ahlstrom et al. (1977), among others, used the attractive random walk model to describe the movement of individual solute particles by viewing the travel distance for a particular time step as the sum of a deterministic and a stochastic velocity component.

In the following, only a brief introduction to the finite difference and finite element methods to solve transport problems is provided. Both methods encompass a wide variety of more specific numerical approaches. As a rule of thumb, the finite difference method is attractive because of its simplicity and the availability, at least early on, of handbooks and computer programs simulating flow and transport in porous media. On the other hand, the finite element method has proven to be more suitable for problems involving irregular geometries of the flow and transport problem, such as situations involving flow to drainage pipes and along sloping soil surfaces.

6.3.3.2 Finite Difference Methods

For one-dimensional transient solute transport the dependent variable $[C(x,t)]$ can be discretized according to

$$C(x,t) = C(i\Delta x, j\Delta t) = C_{ij} \qquad (i = 0,1,2,....,n; j = 0,1,2,....,m) \qquad [6.98]$$

Consider the simulation of the one-dimensional ADE for steady flow of a conservative tracer as given by Equation [6.63] with $R = 1$. Temporal and spatial derivatives are approximated with Taylor series expansions. Assume that the concentrations are known at the current time $(t = j\Delta t)$ and that the objective is to calculate the concentration distribution $\{C[i\Delta x,(j+1)t]\}$ at the next time. A forward-in-time finite difference scheme where the unknown concentration is given explicitly in terms of known concentrations, is written as

$$\frac{C_{i,j+1} - C_{i,j}}{\Delta t} \approx D \frac{C_{i+1,j} - 2C_{i,j} + C_{i-1,j}}{(\Delta x)^2} - v \frac{C_{i+1,j} - C_{i-1,j}}{2\Delta x} \qquad [6.99]$$

On the other hand, a backward-in-time or implicit scheme is given by:

$$\frac{C_{i,j+1} - C_{i,j}}{\Delta t} \approx D \frac{C_{i+1,j+1} - 2C_{i,j+1} + C_{i-1,j+1}}{(\Delta x)^2} - v \frac{C_{i+1,j+1} - C_{i-1,j+1}}{2\Delta x} \qquad [6.100]$$

which contains several concentrations at the next time level. The problem is solved implicitly after combining the difference schemes of all nodes, and subsequently using a matrix equation solver. Finally, a weighted scheme can be defined as:

$$\frac{C_{i,j+1} - C_{i,j}}{\Delta t} \approx D \frac{\omega\left(C_{i+1,j+1} - 2C_{i,j+1} + C_{i-1,j+1}\right) + (1-\omega)\left(C_{i+1,j} - 2C_{i,j} + C_{i-1,j}\right)}{(\Delta x)^2}$$

$$-v \frac{\omega\left(C_{i+1,j+1} - C_{i-1,j+1}\right) + (1-\omega)\left(C_{i+1,j} - C_{i-1,j}\right)}{2\Delta x} \qquad [6.101]$$

in which ω is a weighting constant between 0 and 1. The scheme is said to be fully explicit for $\omega = 0$ and fully implicit for $\omega = 1$, while a Crank-Nicolson central-in-time scheme is derived if $\omega = 0.5$. For transient flow, the scheme becomes more complicated; the velocity (v) and water content (θ) are usually obtained by solving the Richards equation prior to solving the transport problem.

Errors associated with the discretization and the solution procedure can be evaluated by comparison to analytical results, provided that the problem can be sufficiently idealized (linearized) to permit the use of such solutions. This is true for other numerical solutions as well. For a convergent scheme, the difference between the numerical and analytical solutions should decrease if smaller space and time steps are used in the numerical solution; the difference should become zero if $\Delta x \to 0$ and $\Delta t \to 0$, barring round off and computational errors.

An even more important question relates to the stability of the finite difference approximation, namely, the degree to which the numerical solution is affected by errors that occur during the simulation. Such errors can usually not be eliminated completely; they depend on the implemented discretization, the values of the input parameters, and the type of numerical scheme used for approximation of the governing transport equation. Errors are damped during the course of a simulation when a stable scheme is used, while unstable schemes allow such errors to grow unboundedly.

Implicit systems are unconditionally stable, but their results may not be as amenable to changes in grid sizes as is the case with explicit systems. The Crank-Nicolson method offers an attractive compromise of being unconditionally stable and having a truncation error of order $O[(\Delta x)^2 + (\Delta t)^2]$. These properties imply, among other things, that a variable time step can be used independently of the spatial step to effectively balance the needs of an accurate approximation and a limited number of computations. However, oscillations near the concentration front may develop even for unconditionally stable methods due to the hyperbolic (convection) term in the solute transport equation. To avoid these oscillations, stability criteria in terms of the grid Peclet (P or Pe) and Courant (Cr) numbers are frequently formulated. Huyakorn and Pinder (1983) provided the following conservative guidelines for one-dimensional transport of a nonreactive solute:

$$Pe = v\Delta x / D < 2 \qquad [6.102]$$

$$Cr = v\Delta t / \Delta x < 1$$

[6.103]

For transport of a reactive solute, the retardation factor R must be included in the denominator of the Courant number.

6.3.3.3 Finite Element Methods

The application of the finite element methods for modeling solute transport in soils involves several steps, which will be briefly reviewed in a qualitative manner. The specifics of the method can be found in, among others, Huyakorn and Pinder (1983) and Istok (1989). The (spatial) solution domain should first be discretized. The finite element mesh, consisting of nodal points marking the elements, is usually tailored to the problem at hand. The selection of mesh size is a somewhat subjective process that considers the required degree of accuracy, the geometry of the problem, the ease of mesh generation, and the mathematical complexity associated with the use of a particular mesh. The shape of the finite elements is determined by the dimensionality and the geometry of the transport problem. One-dimensional elements consist of lines between nodal points along the coordinate where (one-dimensional) transport occurs. Examples of two-dimensional elements are triangles, rectangles, and parallelograms, while many different three-dimensional elements can be constructed.

A second step in implementing the finite element method is the description of the transport problem for each element. Generally, the method of weighted residuals is used to arrive at an integral formulation for the governing transport equation. An approximate or trial solution for the concentration in each element is formulated as the weighted sum of the unknown concentration at the nodes of that element. A wide variety of so-called basis functions can be selected to assign weights to the nodes; the functions depend on the type of element being selected. The approximation for the element concentration will not be exact; substitution of the element concentration in the ADE yields an expression for this error (residual). The objective is to minimize the residual over the entire domain with some kind of weighting procedure for the elements. The method of weighted residuals forces the weighted average of the residuals at the nodes to be zero and gives an expression for the residual of each element. After applying Green's theorem for each element, the residual can be written in matrix form.

The third step is the assembly of all element matrices into a global matrix system that contains the nodal concentrations and its temporal derivative as unknown variables.

The last step involves the solution of this global matrix equation. Since there are, in general, no obvious advantages for also using a finite element approximation for the temporal derivative, the latter is normally dealt with using the (simpler) finite difference method. The time step may be constant or variable. As noted earlier, the explicit or forward scheme ($\omega = 0$) is conditionally stable whereas the implicit or backward ($\omega = 1$) and the centered or Crank-Nicolson ($\omega = 0.5$) schemes are uncon-ditionally stable. The nodal concentration can then be solved using standard numerical procedures.

6.3.3.4 Application

Numerical oscillations and dispersion are illustrated for several numerical schemes using results by Huang et al. (1997). The numerical solution of the ADE is particularly difficult for relatively sharp concentration fronts with advection-dominated transport characterized by small dispersivities. As mentioned earlier, undesired oscillations can often be prevented with judicious space and time discretizations. The Peclet number increases when advection dominates dispersion; the potentially adverse effect on the numerical solution can be compensated by selecting a smaller grid size. Numerical oscillations can be virtually eliminated if the local Peclet number is always less than 2.

However, acceptable results may still be obtained for local Peclet numbers as high as 10 (Huyakorn and Pinder, 1983). The time discretization is based on a second dimensionless number, the Courant number (Equation [6.103]).

Consider one-dimensional, steady-state flow in a soil column with $v = 4$ cm d^{-1}. The column was initially free of any solute, a nonreactive solute ($C_o = 1$) was subsequently applied for 20 days. For negligible molecular diffusion and a longitudinal dispersivity ($\alpha_L = 0.02$ cm), the grid Peclet for a spatial discretization ($\Delta x = 2$ cm) is given by:

$$Pe = \frac{v\Delta x}{D} = \frac{\Delta x}{\alpha_L} = 100$$

[6.104]

This grid Peclet number of 100 indicates solute transport that is dominated by advection. In all calculations, the Courant number was less than 1, which is the stability condition for Eulerian methods.

The concentration predicted with four different finite element methods and with the analytical solution is shown in Fig. 6.13. The first numerical method is based on the central Crank-Nicolson scheme for time with weighting constant ($\omega = 0.5$). Second, the analytical solution is shown as a solid line. Third, an implicit scheme ($\omega = 1.0$) is used. The last two numerical methods implement upstream weighting (Huyakorn and Pinder, 1983) in the central and the implicit schemes, respectively. The results obtained with the Crank-Nicolson method have significant numerical oscillations (both overshoot and undershoot) (Fig. 6.13). This is not surprising given the large value for Pe. The oscillations are reduced by using an implicit scheme. Upstream weighting leads to very similar results for the central and implicit schemes. The oscillations are virtually eliminated but the solute profile exhibits more numerical dispersion; there is a greater discrepancy with the steep analytical profile than for the regular implicit scheme.

6.4 Stream Tube Models

Considerable errors may be made when applying deterministic methods to the field since model parameters are actually stochastic due to spatial and temporal variability, measurement errors, and different averaging scales. Usually, it is not possible or important to obtain discrete values for parameters in deterministic models of field-scale transport. Instead, transport properties and model results are described with statistical functions. Stochastic modeling is no substitute for data collection or model development, but merely a method to deal with uncertainty of model parameters and complexity of flow and transport processes. The scale at which solute movement is observed or modeled is important. The averaging process associated with larger field-scale descriptions tends to filter out the variability at smaller scales.

The stochastic modeling of actual field problems is seldom possible. The stream tube model provides a possible exception (Dagan and Bresler, 1979; Amoozegar-Fard et al., 1982; Rubin and Or, 1993). The field is conceptualized as a system of parallel tubes illustrated in Fig. 6.14. A process-based model is used to describe a one-dimensional, autonomous transport in each tube as a function of time and depth. Transport parameters are either deterministic or stochastic. The problem may be solved analytically at the scale of the tube and the field. The stream tube model is suitable for inverse procedures to estimate transport and statistical properties (Toride et al., 1995).
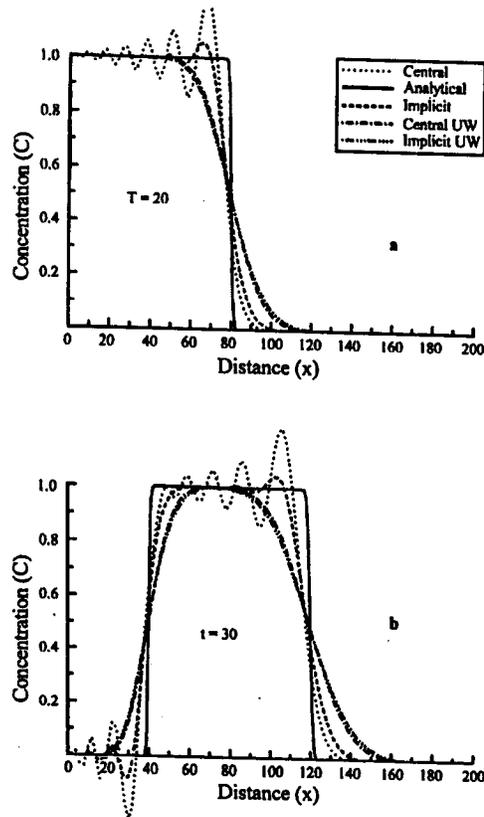
Fig. 6.13 Concentration profiles predicted with different numerical schemes for (a) solute infiltration ($t = 30$ d) and (b) solute leaching ($t = 30$ d)
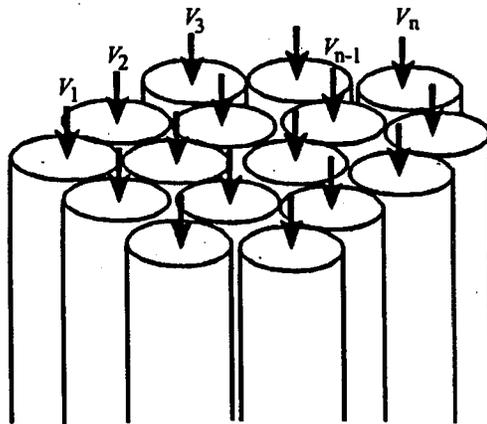

Fig. 6.14 Schematic of the stream tube model

6.4.1 Model Formulation

For one-dimensional transport, the solute concentration at the outlet of a stream tube of length (L) may be written with the transfer function approach as (Jury and Roth, 1990):

$$C(L,t) = \int_0^t C(0, t - \tau) f(L, \tau) d\tau$$

[6.105]

The outlet concentration is a convolution of the input signal and the residence time distribution $f(L, \tau)$. The latter is, in effect, a probability density function (pdf) of the time a solute particle resides in the soil between $x = 0$ and L. The pdf, which has dimension of inverse time, can be determined from experimental results or it may be a theoretical expression derived from a process-based model such as the ADE. The pdf depends mostly on the transport properties of the soil, it depends to some degree on the mode of solute application and detection, but not on the input and initial concentrations. For the equilibrium problem involving instantaneous solute application to a solute-free soil, the flux-averaged concentration and hence the pdf is given by:

$$f(x,t) = \frac{x}{\sqrt{4\pi D t^3}} \exp\left(-\frac{(x - vt)^2}{4Dt}\right)$$

[6.106]

Note that this is a Gaussian pdf. Expressions for $f(x,t)$ derived at a particular depth can be readily used for predicting concentrations at other depths if the soil is homogeneous.

The stochastic approach is implemented by considering the (constant) column parameters as realizations of a random distribution. The (horizontal) field-averaged solute concentration is considered the ensemble average over the probability distribution. It is assumed that each random parameter obeys a distribution function that is independent of location and that the ensemble of possible concentrations may be estimated from a sufficient number of samples taken at different locations. The average concentration across the field is then identical to the ensemble average:

$$\langle C(x,t) \rangle = \frac{1}{A} \int_A C(x,t) dA = \lim_{n \to \infty} \frac{1}{n} \sum_{i=1}^{n} C_i(x,t)$$

[6.107]

where A denotes the area of the field, n is the number of samples, and $< >$ indicates an ensemble average.

6.4.2 Application

Solute transport in a local-scale stream tube may be described with the one-dimensional ADE. Following Toride and Leij (1996a), the effects of heterogeneity are studied using pairs of random parameters $(v$ and $K_d)$. Note that the water content (θ) and bulk density (ρ_b) are the same for all stream tubes. The field-scale mean concentration (denoted by ^) is equal to the ensemble average:

$$\hat{C}(x,t) = \langle C(x,t) \rangle = \int_0^\infty \int_0^\infty C(x,t; v, K_d) f(v, K_d) dv \, dK_d$$

[6.108]

where the bivariate lognormal joint probability density function $f(v, K_d)$ is given by:

$$f(v, K_d) = \frac{1}{2\pi\sigma_v\sigma_{Kd}vK_d\sqrt{1-\rho_{vKd}^2}} \ \exp\left(-\frac{Y_v^2 - 2\rho_{vKd}Y_vY_{Kd} + Y_{Kd}^2}{2(1-\rho_{vKd}^2)}\right)$$

[6.109]

with

$$\rho_{vKd} = \langle Y_vY_{Kd} \rangle = \int_0^\infty \int_0^\infty Y_vY_{Kd}f(v, K_d)dv\, dK_d$$

[6.110]

$$Y_v = \frac{\ln(v) - \mu_v}{\sigma_v}, \quad Y_{Kd} = \frac{\ln(K_d) - \mu_{Kd}}{\sigma_{Kd}}$$

[6.111]

where μ and σ are the mean and standard deviation of the log transformed variable, and ρ_{vKd} is the correlation coefficient between Y_v and Y_{Kd} (K_d tends to increase with v for positive ρ_{vKd} while K_d decreases with v for negative ρ_{vKd}). Ensemble averages of v and K_d are given by (Aitcheson and Brown, 1963)

$$\langle v \rangle = \exp\left(\mu_v + \frac{1}{2}\sigma_v^2\right), \quad \langle K_d \rangle = \exp\left(\mu_{Kd} + \frac{1}{2}\sigma_{Kd}^2\right)$$

[6.112]

with coefficients of variation (CV):

$$CV(v) = \sqrt{\exp(\sigma_v^2) - 1}, \quad CV(K_d) = \sqrt{\exp(\sigma_{Kd}^2) - 1}$$

[6.113]

Based upon the detection mode of the local-scale concentration, three types of field-scale concentrations can be defined: (1) the ensemble average of the flux-averaged concentration ($<C_F>$); (2) the field-scale resident concentration ($\hat{C}_R$), which is equal to the ensemble average of the resident concentration ($<C_R>$); and (3) the field-scale flux-averaged concentration ($\hat{C}_F$) which is defined as $<vC_F>/<v>$. The second type of concentration is obtained from averaging values of the resident concentration at a particular depth across the field. The third type is defined as the ratio of ensemble solute and water fluxes in a similar manner as for deterministic transport. It should be noted that $<vC_F>/<v> \neq <C_F>$ because v is a stochastic variable.

The use of the stream tube model for field-scale transport is illustrated in Fig. 6.15. The local-scale concentration only depends on the particular realizations of the two stochastic parameters (v and K_d) after the independent variables (t and x) have been specified. The solution for the ADE at $x = 100$ cm and $t = 5$ day as a function of v and K_d is shown in Fig. 6.15a and the bivariate lognormal pdf for v and K_d in Fig. 6.15b; the distribution is skewed with respect to v since σ_v is fairly high, the smaller σ_{Kd} results in a more symmetric distribution for K_d. The negative ρ_{vKd} results in an increasing v with a decreasing K_d, and *vice versa*. The expected concentration is shown in Fig. 6.15c, which is obtained by weighting the local concentration (Fig. 6.15a) by multiplying it with the joint pdf (Fig. 6.16b). The peak in Fig. 6.15c suggests that stream tubes with approximately $v = 25$ cm d^{-1} and $K_d = 1$ cm^3 g^{-1} contribute the most to solute breakthrough when $x = 100$ cm and $t = 5$ days. The volume of the distribution in Fig. 6.15c corresponds to the ensemble average ($<C_R>$).

Variations in the local-scale concentration between stream tubes, at a particular depth and time, can be characterized by its variance. The variance across the horizontal plane is given by (Bresler and Dagan, 1981; Toride and Leij, 1996b):
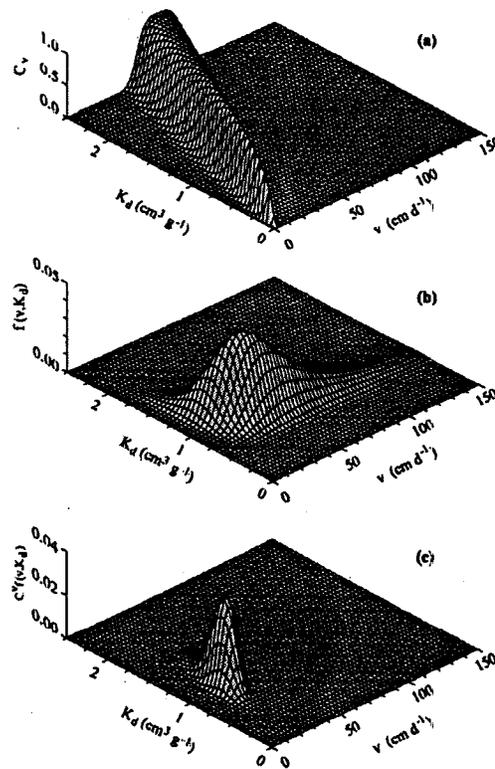
$$Var[C(x,t)] = \int_0^\infty \int_0^\infty [C(x,t) - \langle C(x,t) \rangle]^2 f(v, K_d) dv \, dK_d = \langle C^2(x,t) \rangle - \langle C(x,t) \rangle^2 \quad [6.114]$$

For a deterministic distribution coefficient (K_d) Equation [6.108] reduces to:

$$\langle C(x,t) \rangle = \int_0^\infty C(x,t;v) f(v) dv \quad [6.115]$$

where the lognormal pdf for the single stochastic variable (v) is given by:

$$f(v) = \frac{1}{\sqrt{2\pi}\sigma_v v} \exp\left(-\frac{[\ln(v) - \mu_v]^2}{2\sigma_v^2}\right) \quad [6.116]$$

Fig. 6.15 Illustration of the stream tube model for field-scale transport for a 2-d solute application with $D = 20$ cm^2 d^{-1} and $\rho_b/\theta = 4$ g cm^{-3}: (a) the local-scale concentration, C_R, as a function of v and K_d at $x = 100$ cm and $t = 5$ days; (b) a bivariate lognormal pdf for $\rho_{vKd} = 0.5$, $<v> = 50$ cm d^{-1}, $\sigma_v = 0.2$, $<K_d> = 1$ cm^3 g^{-1}, and $\sigma_{Kd} = 0.2$; and (c) the expected concentration, C^R, at $x = 100$ cm and $t = 5$ days.

The mean (Fig. 6.16a) ($\hat{C}_R = <C_R>$) and the variance (Fig. 6.16b) are shown according to Equation [6.114], as a function of depth for three values of σ_v at $t = 3$ day for a nonreactive solute. More solute spreading occurs in the $\hat{C}_R$-profile when σ_v increases (Figure 6.16a). The variation in the local-scale C_R also increases with σ_v, indicating a more heterogeneous solute distribution in the horizontal plane (Fig. 6.16b). Because flow and transport become more heterogeneous as σ_v increases, more observations are needed to estimate $\hat{C}_R$ for $\sigma_v = 0.5$ than for $\sigma_v = 0.1$. The double peak in the variance profiles of Fig. 6.16b is due to the relative minimum for this pulse application at around $x = 30$ cm, where the highest concentration occurs.

For reactive solutes, the variability in the distribution coefficient (K_d) must also be considered. The field-scale resident concentration ($\hat{C}_R$) at $t = 5$ day is plotted versus depth in Fig. 6.17 for perfect and no correlation between v and K_d. The figure shows that the negative correlation between v and K_d causes additional spreading. Such a negative correlation seems plausible since coarse-textured soils generally have a relatively high v, due to their higher hydraulic conductivity, and a small K_d, due to their lower exchange capacity. The opposite may hold for fine-textured soils. Robin et al. (1991) reported a weak negative correlation between K_d and the saturated hydraulic conductivity for a sandy aquifer.
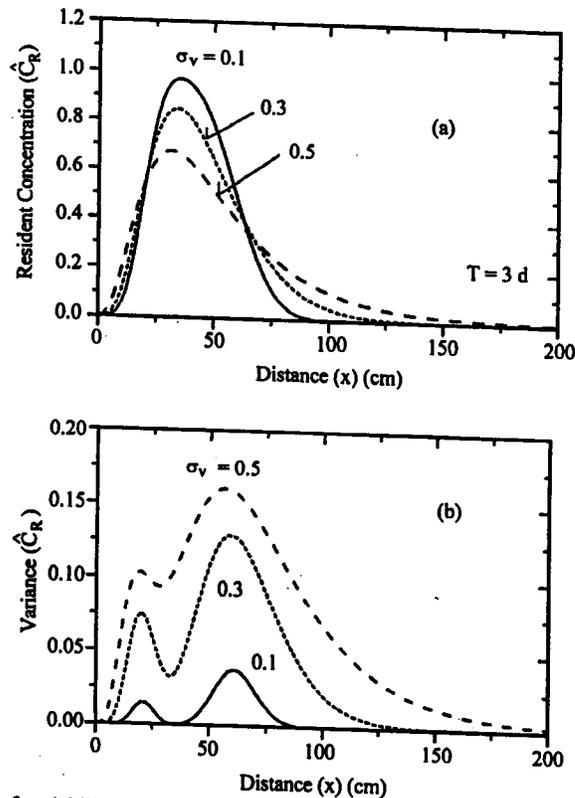
Fig. 6.16 The effect of variability in the pore-water velocity, v, on (a) the field scale resident concentration profile, and (b) the distribution of the variance for $\hat{C}_R$ in the horizontal plane; for a 2-d application of a nonreactive solute (R = 1) assuming $<v> = 20$ cm d^{-1} and $D = 20$ cm^2 d^{-1}
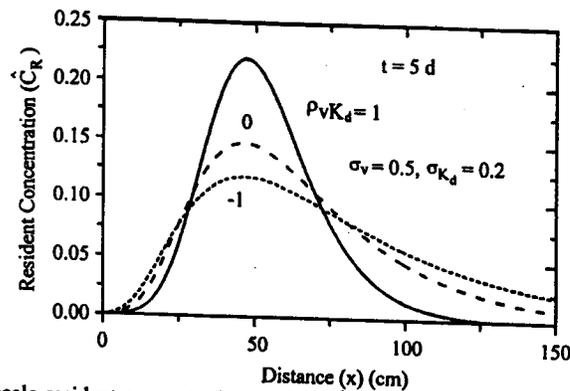
Fig. 6.17 The field-scale resident concentration profile, $\hat{C}_R(x)$, for three different correlations between v and K_d with $<v> = 50$ cm d^{-1}, $D = 20$ cm^{2}d^{-1}, $<K_d> = 1$ g^{-1}cm^3, $\sigma_{K_d} = 0.2$, $<R> = 5$, and $\rho_b/\theta = .4$ g cm^{-3}

6.5 References

Ahlstrom, S.W., H.P. Foote, R.C. Arnett, C.R. Cole, and R.J. Serne. 1977. Multicomponent mass transport model theory and numerical implementation. Battelle Pacific Northwest Laboratory Report BNWL-2127. Richland, WA.

Aitcheson, J., and J.A.C. Brown. 1963. The lognormal distribution. Cambridge University Press. London, UK.

Amoozegar-Fard, A., D.R. Nielsen, and A.W. Warrick. 1982. Soil solute concentration distribution for spatially varying pore water velocities and apparent diffusion coefficients. Soil Sci. Soc. Am. J. 46:3–9.

Aris, R. 1956. On the dispersion of a solute in a fluid flowing through a tube. Proc. Roy. Soc. London Ser. 235:67–77.

Aris, R. 1958. On the dispersion of linear kinematic waves. Proc. Roy. Soc. London Ser. 245:268–277.

Bear, J., and A. Verruijt. 1987. Modeling groundwater flow and pollution. Kluwer Academic Publishers, Norwell, MA.

Boyd, G.E., A.W. Adamson, and L.S. Meyers. 1947. The exchange adsorption of ions from aqueous solutions by organic zeolites. II. Kinetics. J. Am. Chem. Soc. 69:2836–2848.

Brenner, H. 1962. The diffusion model of longitudinal mixing in beds of finite length. Numerical values. Chem. Eng. Sci. 17:229–243.

Bresler, E. 1973. Simultaneous transport of solutes and water under transient unsaturated flow conditions. Water Resour. Res. 9:975–986.

Bresler, E., and G. Dagan. 1981. Convective and pore scale dispersive solute transport in unsaturated heterogeneous fields. Water Resour. Res. 17: 1683–1693.

Bresler, E., and R.J. Hanks. 1969. Numerical method for estimating simultaneous flow of water and salt in saturated soils. Soil Sci. Soc. Am. Proc. 33:827–832.

Campbell, G.S. 1985. Soil physics with BASIC: Transport models for soil-plant systems. Elsevier, New York, NY.

Carslaw, H.S., and J.C. Jaeger. 1959. Conduction of heat in solids. Clarendon Press, Oxford, UK.

Chaudhari, N.M. 1971. An improved numerical technique for solving multidimensional miscible displacement. Soc. Pet. Eng. J. 11:277–284.

Coats, K.H., and B.D. Smith. 1964. Dead end pore volume and dispersion in porous media. Soc. Petrol. Eng. J. 4:73–84.

Crank, J. 1975. The mathematics of diffusion. Clarendon Press, Oxford, UK.

Dagan, G., and E. Bresler. 1979. Solute dispersion in unsaturated heterogeneous soil at field-scale. I. Theory. Soil Sci. Soc. Amer. J. 43:461–467.

Donea, J. 1991. Generalized Galerkin methods for convection dominated transport phenomena. Appl. Mech. Rev. 44:205–214.

Dykhuizen, R.C., and W.H. Casey. 1989. An analysis of solute diffusion in rocks. Geochim. Cosmochim. Acta 53:2797–2805.

Epstein, N. 1989. On tortuosity and the tortuosity factor in flow and diffusion through porous media. Chem. Eng. Sci. 44:777–780.

Fischer, H.B., E. List, R.C.Y. Koh, J. Imberger, and N.H. Brooks. 1979. Mixing in inland and coastal waters. Academic Press, New York, NY.

Fried, J.J., and M.A. Combarnous. 1971. Dispersion in porous media. Adv. Hydrosci. 9:169–282.

Gautschi, W. 1964. Error function and Fresnel integrals. p. 295–329. *In* M. Abramowitz and I.A. Stegun handbook of mathematical functions. Appl. Math. Ser. 55. National Bureau of Standards, Washington, DC.

Gelhar, L.W., C. Welthy, and K.R. Rehfeldt. 1992. A critical review of data on field-scale dispersion in aquifers. Water Resour. Res. 28:1955–1974.

Goldstein, S. 1953. On the mathematics of exchange processes in fixed columns. I. Mathematical solutions and asymptotic expansions. Proc. Roy. Soc. London Ser. A. 219:151–185.

Gray, W.G., and G.F. Pinder. 1976. An analysis of the numerical solution of the transport equation. Water Resour. Res. 12:547–555.

Hamaker, J.W. 1972. Diffusion and volatilization, p. 341–397. *In* C.A.I. Goring and J.W. Hamaker (ed.) Organic chemicals in the soil environment. Marcel Dekker, Inc., New York, NY.

Harvie, C.E., and J.H. Weare. 1980. The prediction of mineral solubilities in natural waters: The Na-K-Mg-Ca-Cl-SO_4-H_2O system from zero to high concentration at 25 C. Geochim. Cosmochim. Acta 44:981–997.

Helfferich, F. 1962. Ion exchange. McGraw-Hill. New York, NY.

Huang, K., and M. Th. van Genuchten. 1995. An analytical solution for predicting solute transport during ponded infiltration. Soil Sci. 159:217–223.

Huang, K., J. Šimunek, and M. Th. van Genuchten. 1997. A third-order numerical scheme with upwind weighting for modeling solute transport. Int. J. Numer. Meth. Eng. 40:1623–1637.

Huyakorn, P.S., and G.F. Pinder. 1983. Computational methods in subsurface flow. Academic Press, New York, NY.

Istok, J. 1989. Groundwater modeling by the finite element method. American Geophysical Union, Washington, DC.

Jacobsen, O.H., F.J. Leij, and M. Th. van Genuchten. 1992. Parameter determination for chloride and tritium transport in undisturbed lysimeters during steady flow. Nordic Hydrol. 23:89–104.

Jin, Y., and W.A. Jury. 1996. Characterizing the dependence of gas diffusion coefficient on soil properties. Soil Sci. Soc. Am. J. 60:66–71.

Jury, W.A., and K. Roth. 1990. Transfer functions and solute movement through soil. Theory and applications. Birkhäuser Verlag, Basel, Switzerland.

Kemper, W.D. 1986. Solute Diffusivity. p. 1007–1024. *In* A. Klute (ed.) Methods of soil analysis. I. Physical and mineralogical methods. Soil Science Society of America, Madison, WI.

Klotz, D., K.P. Seiler, H. Moser, and F. Neumaier. 1980. Dispersivity and velocity relationship from laboratory and field experiments. J. Hydrol. 45:169–184.

Konikov, L.F., and J.D. Bredehoeft. 1978. Computer model of two-dimensional solute transport and dispersion in groundwater. *In* Techniques of water resources investigation, Book 7. US Geological Survey, Reston, VA.

Kreft, A., and A. Zuber. 1978. On the physical meaning of the dispersion equations and its solutions for different initial and boundary conditions. Chem. Eng. Sci. 33:1471–1480.

Kreft, A., and A. Zuber. 1986. Comments on "Flux-averaged and volume-averaged concentrations in continuum approaches to solute transport" by J. C. Parker and M. Th. van Genuchten. Water Resour. Res. 22:1157–1158.

Krupp, H.K., J.W. Biggar, and D.R. Nielsen. 1972. Relative flow rates of salt and water in soil. Soil Sci. Soc. Amer. Proc. 36:412–417.

Lassey, K.R. 1988. Unidimensional solute transport incorporating equilibrium and rate-limited isotherms with first-order loss. 1. Model conceptualizations and analytic solutions. Water Resour. Res. 3:343–350.

Leij, F.J., and J.H. Dane. 1992. Moment method applied to solute transport with binary and ternary exchange. Soil Sci. Soc. Am. J. 56:667–674.

Leij, F.J., and N. Toride. 1995. Discrete time- and length-averaged solutions of the advection-dispersion equation. Water Resour. Res. 31:1713–1724.

Leij, F.J., and M. Th. van Genuchten. 1995. Approximate analytical solutions for transport in two-layer porous media. Trans. Porous Media 18:65–85.

Li, S-G, F. Ruan, and D. McLaughlin. 1992. A space-time accurate method for solving solute transport problems. Water Resour. Res. 28:2297–2306.

Lide, D.R. 1995. Handbook of chemistry and physics. CRC Press, Boca Raton, FL.

Lindstrom, F.T., and M.N.L. Narasimhan. 1973. Mathematical theory of a kinetic model for dispersion of previously distributed chemicals in a sorbing porous medium. SIAM J. Appl. Math. 24:469–510.

Lindstrom, F.T., and W.M. Stone. 1974. On the start up or initial phase of linear mass transport of chemicals in a water saturated sorbing porous medium. SIAM J. Appl. Math. 26:578–591.

Millington, R.J. 1959. Gas diffusion of porous solids. Science 130:100–102.

Millington, R.J., and J.P. Quirk. 1961. Permeability of porous solids. Trans. Farad. Soc. 57:1200–1206.

Molz, F.J., M.A. Widdowson, and L.D. Benefield. 1986. Simulation of microbial growth dynamics coupled to nutrient and oxygen transport in porous media. Water Resour. Res. 22:1207–1216.

Moridis, G.J., and D.L. Reddell. 1991. The Laplace transform finite difference method for simulation of flow through porous media. Water Resour. Res. 27:1873–1884.

Nauman, E.B., and B.A. Buffham. 1983. Mixing in continuous flow systems. John Wiley and Sons, New York, NY.

Neuman, S.P. 1984. Adaptive Eulerian-Lagrangian finite element method for advection-dispersion. Int. J. Numer. Meth. Eng. 20:321–337.

Nielsen, D.R., and J.W. Biggar. 1961. Miscible displacement in soils. I. Experimental information. Soil Sci. Soc. Amer. Proc. 25:1–5.

Nkedi-Kizza, P., J.W. Biggar, M. Th. van Genuchten, P.J. Wierenga, H.M. Selim, J.M. Davidson, and D.R. Nielsen. 1983. Modeling tritium and chloride 36 transport through an aggregated oxisol. Water Resour. Res. 19:691–700.

Nkedi-Kizza, P., J.W. Biggar, H.M. Selim, M. Th. van Genuchten, P.J. Wierenga, J.M. Davidson, and D.R. Nielsen. 1984. On the equivalence of two conceptual models for describing ion exchange during transport through an aggregated Oxisol. Water Resour. Res. 20:1123–1130.

Nye, P.H. 1979. Diffusion of ions and uncharged solutes in soils and soil clays. Adv. Agron. 31: 225–272.

Olsen, S.R., and W.D. Kemper. 1968. Movement of nutrients to plant roots. Adv. Agron. 20:91–151.

Oscarson, D.W., H.B. Hume, N.G. Sawatsky, and S.C.H. Cheung. 1992. Diffusion of iodide in compacted bentonite. Soil Sci. Soc. Am. J. 56:1400–1406.

Parker, J.C., and M. Th. van Genuchten. 1984a. Flux-averaged concentrations in continuum approaches to solute transport. Water Resour. Res. 20:866–872.

Parker, J.C., and M. Th. van Genuchten. 1984b. Determining transport parameters from laboratory and field tracer experiments. VA Agric. Exp. Stat. Bull. 84–3.

Pinder, G.F., and W.G. Gray. 1977. Finite elements in surface and subsurface hydrology. Academic Press, New York, NY.

Pitzer, K.S. 1979. Activity coefficients in electrolyte solutions. CRC Press, Boca Raton, FL.

Robin, M.J.L., R.W. Gillham, and D.W. Oscarson. 1987. Diffusion of strontium and chloride in compacted clay-based materials. Soil Sci. Soc. Am. J. 51:1102–1108.

Robin, M.J.L., E.A. Sudicky, R.W. Gillham, and R.G. Kachanoski. 1991. Spatial variability of Strontium distribution coefficients and their correlation with hydraulic conductivity in the Canadian Forces Base Borden aquifer. Water Resour. Res. 27: 2619– 2632.

Rubin, Y., and D. Or. 1993. Stochastic modeling of unsaturated flow in heterogeneous soils with water uptake by plant roots: The parallel columns model. Water Resour. Res. 29:619–631.

Scheidegger, A.E. 1974. The physics of flow through porous media. University of Toronto Press, Toronto, Canada.

Selim, H.M., J.M. Davidson, and R.S. Mansell. 1976. Evaluation of a two-site adsorption-desorption model for describing solute transport in soil. p. 444–448. In Proc. Computer Simulation Conference, American Institute of Chemical Engineering, Washington, DC.

Selim, H.M., and R.S. Mansell. 1976. Analytical solution of the equation for transport of reactive solutes through soils. Water Resour. Res. 12:528–532.

Simon, W., P. Reichert, and C. Hinz. 1997. Properties of exact and approximate traveling wave solutions for transport with nonlinear and nonequilibrium sorption. Water Resour Res. 33:1139–1147.

Sparks, D.L. 1989. Kinetics of soil chemical processes. Academic Press, San Diego, CA.

Spiegel, M.R. 1965. Theory and problems of Laplace transforms. Schaum's Outline Series, McGraw-Hill, New York, NY.

Sudicky, E.A. 1989. The Laplace transform Galerkin technique: A time-continuous finite element theory and application to mass transport in groundwater. Water Resour. Res. 25:1833–1846.

Taylor, G.I. 1953. Dispersion of soluble matter in solvent flowing through a tube. Proc. Roy. Soc. London Ser. 219:186–203.

Toride, N., and F.J. Leij. 1996a. Convective-dispersive stream tube nodel for field-scale solute transport: I. Moment analysis. Soil Sci. Soc. Am. J. 60:342–352.

Toride, N., and F.J. Leij. 1996b. Convective-dispersive stream tube nodel for field-scale solute transport: II. Examples and calibration. Soil Sci. Soc. Am. J. 60:352–361.

Toride, N., F.J. Leij, and M. Th. van Genuchten. 1993. A comprehensive set of analytical solutions for nonequilibrium solute transport with first-order decay and zero-order production. Water Resour. Res. 29:2167–2182.

Toride, N., F.J. Leij, and M. Th. van Genuchten. 1994. Flux-averaged concentrations for transport in soils having nonuniform initial solute distributions. Soil Sci. Soc. Am. J. 57:1406–1409.

Toride, N., F.J. Leij, and M. Th. van Genuchten. 1995. The CXTFIT code for estimating transport parameters from laboratory or field tracer experiments. Version 2.0. US Salinity Lab. Res. Rep. 137, Riverside, CA.

van der Heijde, P., Y. Bachmat, J. Bredehoeft, B. Andrews, D. Holtz, and S. Sebastian. 1985. Groundwater management: The use of numerical models. 2nd Ed. American Geophysical Union, Wahington, DC.

van der Laan, E.T. 1958. Notes on the diffusion-type model for the longitudinal mixing in flow. Chem. Eng. Sci. 7:187–191.

van der Zee, S.E.A.T.M. 1990. Analytical traveling wave solutions for transport with nonlinear and nonequilibrium adsorption. Water Resour. Res. 26:2563–2578.

van Genuchten, M. Th. 1978. Mass transport in saturated-unsaturated media. One-dimensional solutions. Princeton University Research Rep. 78-WR-11.

van Genuchten, M. Th. 1981. Non-equilibrium transport parameters from miscible displacement experiments. US Salinity Lab. Res. Rep. 119, Riverside, CA.

van Genuchten, M. Th. 1988. Solute transport. p. 360-362. In S.P. Parker (ed.) McGraw-Hill Yearbook of Science and Technology, McGraw-Hill Book Co., New York, NY.

van Genuchten, M. Th., and W.J. Alves. 1982. Analytical solutions of the one-dimensional convective-dispersive solute transport equation. USDA Tech. Bull. 1661.

van Genuchten, M. Th., and R.W. Cleary. 1982. Movement of solutes in soils: Computer-simulated and laboratory results. p. 349-386. In G.H. Bolt (ed.). Soil Chemistry. B. Physico-chemical models. Elsevier. Amsterdam, Netherlands.

van Genuchten, M. Th., and F.N. Dalton. 1986. Models for simulating salt movement in aggregated field soils. Geoderma 38:165–183.

van Genuchten, M. Th., and W.G. Gray. 1978. Analysis of some dispersion corrected numerical schemes for solution of the transport equation. Int. J. Num. Meth. Eng. 12:387–404.

van Genuchten, M. Th., and J.C. Parker. 1987. Parameter estimation for various contaminant transport models, p. 273–295. In C.A. Brebbia and G.A. Keramidas (ed.) Reliability and robustness of engineering software. Elsevier, New York, NY.

van Genuchten, M. Th., and J.C. Parker. 1984. Boundary conditions for displacement experiments through short laboratory columns. Soil Sci. Soc. Amer. J. 48:703–708.

van Genuchten, M. Th., and E.A. Sudicky. 1999. Recent advances in vadose zone flow and transport modeling. p. 155–193. In M.B. Parlange and J.W. Hopmans (ed.) Vadose zone hydrology: Cutting across disciplines. Oxford University Press, New York, NY.

van Genuchten, M. Th., D.H. Tang, and R. Guennelon. 1984. Some exact solutions for solute transport through soils containing large cylindrical macropores. Water Resour. Res., 20:335–346.

van Genuchten, M. Th., and P.J. Wierenga. 1976. Mass transfer studies in sorbing porous media. I. Analytical solutions. Soil Sci. Soc. Amer. J. 40:473–480.

van Genuchten, M. Th., and P.J. Wierenga. 1986. Solute dispersion coefficients and retardation factors. In A. Klute (ed.) Methods of soil analysis. I. Physical and mineralogical methods. Soil Science Society of America, Madison, WI.

van Rees, K.C.J., E.A. Sudicky, P.S.C. Rao, and K.R. Reddy. 1991. Evaluation of laboratory techniques for measuring diffusion coefficients in sediments. Env. Sci. Tech. 25:1605–1611.

Varoglu, E., and W.D.L. Finn. 1982. Utilization of the method of characteristics to solve accurately two-dimensional transport problems by finite elements. Int. J. Num. Fluids 2:173–184.

Wierenga, P.J. 1977. Solute distribution profiles computed with steady-state and transient water movement. Soil Sci. Soc. Amer. J. 41:1050–1055.

Yeh, G.T. 1990. A Lagrangian-eulerian method with zoomable hidden fine-mesh approach to solving advection-dispersion equations. Water Resour. Res. 26:1133–1144.

Yeh, G.T., and V.S. Tripathi. 1989. A critical evaluation of recent developments in hydrogeochemical transport models of reactive multichemical components. Water Resour. Res. 25:93–108.

Yeh, G.T., and V.S. Tripathi. 1991. A model for simulating transport of reactive multispecies components: Model development and demonstration. Water Resour. Res. 27:3075–3094.

Zwillinger, D. 1989. Handbook of differential equations. Academic Press, San Diego, CA.